molecular microbiology

Characterization of *Helicobacter pylori* HP0231 (DsbK): role in disulfide bond formation, redox homeostasis and production of Helicobacter cystein-rich protein HcpE

Journal:	*Molecular Microbiology*
Manuscript ID:	MMI-2014-14548.R1
Manuscript Type:	Research Article
Date Submitted by the Author:	n/a
Complete List of Authors:	Lester, Jeffrey; Western University, Microbiology and Immunology Kichler, Sari; Western University, Microbiology and Immunology Oickle, Brandon; Western University, Microbiology and Immunology Fairweather, Spencer; Western University, Microbiology and Immunology Oberc, Alexander; Western University, Microbiology and Immunology Chahal, Jaspreet; Western University, Microbiology and Immunology Ratnayake, Dinath; Western University, Microbiology and Immunology Creuzenet, Carole; Western University, Microbiology and Immunology
Key Words:	Helicobacter pylori, Disulfide bonds., Dsb proteins., Helicobacter Cysteine-rich proteins. , Protein secretion

Characterization of *Helicobacter pylori* HP0231 (DsbK): role in disulfide bond formation, redox homeostasis and production of Helicobacter cystein-rich protein HcpE.

Lester J.[1]; Kichler S.[1]; Oickle B; Fairweather S.; Oberc A.; Chahal J.; Ratnayake D.; and Creuzenet C.[2].

Western University, Microbiology and Immunology, London, Canada.

[1]: Equal contribution.

[2]: Corresponding author: Western University, Microbiology and Immunology, DSB 3031, London, Ontario, N6A 5C1, Canada. Tel: 1 519 661 3204. Fax: 1 519 661 3499. E-mail: ccreuzen@uwo.ca.

Running title: Characterization of *Helicobacter pylori* DsbK

Key words: *Helicobacter pylori*. Disulfide bonds. Dsb proteins. Helicobacter Cysteine-rich proteins. Protein secretion.

Summary:

H. pylori is a human gastric pathogen that colonizes ~ 50% of the world's population. It can cause gastritis, gastric or duodenal ulcers and also gastric cancer. The numerous side effects of available treatments and the emergence of antibiotic resistant strains are severe concerns that justify further research into *H. pylori*'s pathogenic mechanisms. *H. pylori* produces secreted proteins which may play a role in virulence, including the Helicobacter cysteine rich protein HcpE (a.k.a. HP0235). We demonstrate herein that HcpE is secreted in the culture supernatant both as a soluble protein and in association with outer membrane vesicles. We show that the structure of HcpE comprises an organized array of disulfide bonds. We identify DsbK (a.k.a. HP0231) as a folding factor necessary for HcpE production and secretion in *H. pylori* and show that recombinant DsbK can interact with and refold unprocessed, reduced HcpE *in vitro*. These experiments highlight the first biologically relevant substrate for DsbK. Furthermore, we show that DsbK has DiSulfide Bond (Dsb) forming activity on reduced lysozyme and demonstrate a DsbA-type of activity for DsbK upon expression in *E. coli*, despite its similarity with DsbG. Finally, we show a role of DsbK in maintaining redox homeostasis in *H. pylori*.

Introduction:

Helicobacter pylori is a bacterium that chronically infects ~50% of the world population and causes symptoms ranging from mild gastritis to gastric ulcers and cancers (Uemura *et al.*, 2001; Watanabe *et al.*, 1998). Prevalence in Canada is ~35% (Goodman *et al.*, 2008) but reaches 95% in Northern Aboriginal populations (Cheung *et al.*, 2008). Infection is usually contracted at a young age (Sinha *et al.*, 2004) and can complicate health issues related to poor nutritional conditions, such as the widespread iron deficiency and anemia seen in First Nations and Inuit communities in Canada (Christofides *et al.*, 2005; Goodman *et al.*, 2008). *H. pylori*-mediated chronic gastritis leads to inflammation and atrophy of the stomach epithelium, which can lead to ulceration. Over 65% of gastric ulcers are due to *H. pylori* and peptic ulcers develop in 10% of infected individuals, at an annual cost estimated by the Center for Disease Control at ~$6 billion in the United States for peptic ulcer disease alone (www.cdc.gov/ulcer/economic.htm). Likewise, the chronic inflammation induced by the bacterium is the main trigger of gastric cancers (Rogers *et al.*, 2005; Uemura *et al.*, 2001; Watanabe *et al.*, 1998). *H. pylori* is responsible for ~65 and 80% of gastric cancers in developed and developing countries, respectively (Helicobacter and Cancer Collaborative Group, 2001) and is therefore classified as a Type I carcinogen (Parkin *et al.*, 2005). The risk of gastric cancer increases ~6-fold after *H. pylori* infection (Naumann and Crabtree, 2004), and gastric cancer develops in ~2% of infected patients each year (Helicobacter and Cancer Collaborative Group, 2001; Kusters *et al.*, 2006; Uemura *et al.*, 2001). Because of the very high prevalence of *H. pylori*, this also results in large economic and health burdens. With about a million new cases yearly worldwide, gastric cancer ranks fourth in prevalence worldwide. Prognosis for gastric cancer patients is very poor so that gastric cancer is second for the yearly number of death by cancer worldwide (Ferlay *et al.*, 2010; Forman and Burley, 2006; Parkin *et al.*, 2005).

Anti-*H. pylori* treatments involve at least two antibiotics in high doses and a proton pump inhibitor. Their numerous side effects lead to poor patient compliance, which contributes to the

emergence of antibiotic resistance in *H. pylori* (Albert *et al.*, 2005; Raymond *et al.*, 2010). As a result, treatment failure rates are high, ranging from 13 to 77% (depending on colonizing strain) in Canadian Aboriginals (Goodman *et al.*, 2008). This confounds problems of high *H. pylori* prevalence in these communities: ~95% versus ~35% nationally (Albert *et al.*, 2005; McMahon *et al.*, 2003; Urgesi *et al.*, 2011). Hence, efficient management of *H. pylori* infections and novel treatments are paramount to prevent the development of gastric ulcers and fatal gastric cancer and alleviate co-morbidity issues.

H. pylori produces an extensive arsenal of virulence factors (reviewed in (Backert and Clyne, 2011; Basso *et al.*, 2010; Yamaoka, 2010)). For example, flagella-mediated motility is essential for host colonization by *H. pylori* and flagellum production requires glycosylation of flagellins by pseudaminic acid (Josenhans *et al.*, 2002; Merkx-Jacques *et al.*, 2004). We have recently revealed that protein glycosylation extends to proteins other than flagellins and may also affect virulence (Hopf *et al.*, 2011). The lipopolysaccharide (LPS) and numerous toxins such as VacA and CagA are also involved in virulence, and their role in elicitation of the tissue inflammation that is typically associated with long term colonization is better understood (Cheng *et al.*, 2002; O'Connor *et al.*, 2011; Puls *et al.*, 2002; Raju *et al.*, 2012). Despite abundant research regarding its virulence factors, the mechanisms of pathogenesis of *H. pylori* are not fully understood and the function of many of its ~ 1,600 proteins is still unknown (Alm *et al.*, 1999; Tomb *et al.*, 1997).

Of relevance to this study is the fact that ~23 % of *H. pylori* proteins are predicted to be secreted (Tomb *et al.*, 1997) and ~ 6% of those are conserved hypothetical proteins that may play a role for interactions with the host and for pathogenicity. However little is known about the mechanisms that govern proper protein folding prior to secretion. This is the case for the Helicobacter Cysteine-rich Proteins (Hcps), which are found in all *H. pylori* genomes sequenced to date (Dumrese *et al.*, 2009). Hcps are also found in related organisms such as Campylobacters and *Wolinella succinogenes* as indicated by BLAST searches (www.ncbi.nlm.nih.gov). In *H. pylori* 26695, the Hcps form a family of 7 proteins that are encoded throughout the genome (Hcp A to G) (Tomb *et al.*, 1997). They share 30-46

% sequence similarity to one another and share an unusually high cysteine content of 4.9 to 5.8 % (Table I). They were initially identified as proteins released in *H. pylori* culture supernatants that were antigenic when injected in rabbits (Cao *et al.*, 1998). Their specific activity is still up for debate, but recent data suggest a role in virulence via interactions with immune cells (Deml *et al.*, 2005; Dumrese *et al.*, 2009; Roschitzki *et al.*, 2011).

The mechanism of secretion of these proteins outside the bacterial cell is unknown but can be inferred based on key sequence and structural features of the Hcps. First, the Hcp proteins contain numerous Sel1-like repeats (SLRs) (Table I) which comprises ~30 amino acids and usually mediate protein/protein interactions (Grant and Greenwald, 1996). Typically, SLRs adopt a conserved structure consisting of two antiparallel α-helices maintained in a V shape by interactions between a few conserved residues (Grant and Greenwald, 1996). Several SLRs stack onto one another to form solenoid proteins (Mittl and Schneider-Brachert, 2007). This stacking conveys structural stability to SLR-containing proteins. Interestingly, in Hcps, the helices of each SLR contain a cysteine (Cys), and crystallography data on HcpB/C have shown that the Cys form disulfide bonds between the two helices of the SLR motif (Luthy et al., 2002, 2004), leading to their V-shape structure. These disulfide bonds have been shown to be very important for the stability of HcpB (Devi *et al.*, 2006). Moreover, Hcps have a signal peptide for Sec secretion into the periplasm. Since Sec secretion involves unfolded proteins (Natale et al., 2008), Hcps likely fold and form their disulfide bonds in the periplasm before final secretion outside of the bacterium. The paradigm established for *Escherichia coli* for the formation of disulfide bonds in the periplasm is that disulfide bond formation involves an oxidative pathway to form disulfide bonds *de novo*, and an isomerization pathway to correct inappropriate bonds (Heras et al., 2009). In *E. coli* and in numerous other bacteria, the oxidative and isomerization pathways involve periplasmic DiSulfide Bond proteins (Dsb), namely DsbA/B for the oxidative pathway and DsbC/D for the isomerisation pathway (Bardwell *et al.*, 1991; Guilhot *et al.*, 1995; Heras *et al.*, 2009). A DsbC homologue, DsbG, is present in *E. coli* but, until recently, no substrate had been

identified for DsbG (Depuydt *et al.*, 2009; Hiniker and Bardwell, 2004). These observations taken together suggest that Hcp proteins may interact with periplasmic Dsb proteins to acquire their structure via formation of correct disulfide bonds between their multiple Cys prior to final secretion to the outside environment. The formation of disulfide bonds of HcpB has been investigated in *E. coli* (Devi and Mittl, 2011), but no data concerning disulfide bond formation of Hcps directly in *H. pylori* are available to the best of our knowledge.

The paradigm described above for *Escherichia coli* is not conserved in all bacteria (Dutton *et al.*, 2008; Jameson-Lee *et al.*, 2011), including in *H. pylori* where no DsbA was identified and 4 potential Dsb proteins were identified: HP0595 as DsbB/DsbI-like, HP0377 as DsbC-like, HP0265 as DsbD-like, and HP0231 as DsbG-like (Kaakoush *et al.*, 2007; Raczko *et al.*, 2005; Tomb *et al.*, 1997). In line with the fact that Dsb proteins are often involved in bacterial pathogenicity (Heras *et al.*, 2009), HP0595 and HP0231 are important for gastric colonization in mice (Godlewska *et al.*, 2006; Sabarth *et al.*, 2002). Recent structural data (Yoon *et al.*, 2011) support our modeling-based prediction of HP0231 as a DsbG homologue, but recent functional data suggest that HP0231 has DsbA-like activity (Roszczenko *et al.*, 2012). Therefore, further investigations are necessary to clarify the issue. Also, while activities could be investigated using a variety of model substrates, no physiological substrate has been identified for any of these *H. pylori* Dsb-like proteins so far.

In this work, we focused on HcpE (corresponding to open reading frame HP0235) which is a conserved hypothetical protein of unknown function exhibiting >94 % sequence identity between the nine sequenced *H. pylori* strains available on the NCBI database (http://blast.ncbi.nlm.nih.gov). With 355 amino acids and 19 cysteines, HcpE is the largest member of the Hcp family and contains the largest number of cysteines. Therefore, Dsb-mediated formation of disulfide bonds can be anticipated to be essential to its folding. In this manuscript, we demonstrate that HcpE is secreted in culture supernatants both as a soluble protein and as an outer membrane vesicle-bound form and report on the modeled structure of HcpE to demonstrate the importance of disulfide bonds for its folding. We

identified HP0231 (renamed DsbK in this manuscript) as an interacting partner that is able to assist its solubilization *in vitro* and that influences its production and secretion *in vivo*, thereby identifying the first physiological substrate for DsbK. We further show that DsbK is involved in disulfide bond formation using surrogate substrates and we show that it behaves more like a DsbA protein than a DsbG protein when expressed in *E. coli*. Finally, we show an important role of DsbK in resistance to oxidoreduction stress in *H. pylori*.

Results:

HcpE is secreted in the culture supernatant by various *H. pylori* strains: HcpE is encoded with a predicted Sec secretion signal peptide (http://www.expasy.org), which suggests export to the periplasm. While HcpA and HcpC have been detected in culture supernatants previously ((Bumann *et al.*, 2002; Cao *et al.*, 1998)), it remained to be demonstrated whether HcpE was also further secreted in the outside milieu in the absence of cell lysis. To determine if HcpE was secreted by *H. pylori* NCTC11637, the bacteria were grown in serum-free broth (Marchini *et al.*, 1995) and the culture supernatant was ultra-centrifuged, precipitated by trichloroacetic acid and analyzed for HcpE by Western blotting. Western blotting was performed using a polyclonal serum raised in rabbits against recombinant HcpE that had been cloned and over-expressed in *E. coli* as a C-terminally hexahistidine tagged protein (HcpE-His) and purified by nickel chelation chromatography. An *hcpE* knockout mutant was produced by disruption of the *hcpE* gene by a kanamycin resistance cassette and served as a negative control for Western blotting purposes. A band migrating at the expected molecular weight of HcpE (~ 40 kDa) was clearly detected in total cells and in culture supernatants of the wild-type strain but was absent in the *hcpE* mutant (Figure 1A). To exclude the possibility that the presence of HcpE in culture supernatants was due to cell lysis, the amount of urease present in the supernatant was monitored by phenol red assay (Clyne *et al.*, 1995; Merkx-Jacques *et al.*, 2004). Since urease is cytoplasmic, its absence from culture supernatants indicates lack of cell lysis. The data show minimal

urease activity in the supernatants of both the wild-type strain and the *hcpE* mutant while abundant urease was present in their cell pellets (Figure 1B). Altogether, these data demonstrate the production and secretion of HcpE by strain NCTC 111637 grown in serum-free conditions.

Similar data were obtained for *H. pylori* strain SS1, a strain of human origin that has been adapted to mice (Lee *et al.*, 1997): HcpE was also detected in the wild-type pellets and supernatants in the absence of any cell lysis while no HcpE was detected in the *hcpE* mutant (Figure 1C and D).

A portion of HcpE is secreted in association with outer membrane vesicles: Ultracentrifugation of culture supernatants (after 12,000 x g centrifugation removal of cells and debris) allowed recovery of a fraction of HcpE in association with membrane fragments as indicated by anti-HcpE Western blot (Figure 2A). These membrane fragments comprised complete lipopolysaccharides (LPS) with O-antigen as judged by silver staining before and after proteolysis by proteinase K (Figure 2B). Comparison of the protein profile of these membrane fragments with those of inner and outer membranes (IM and OM, respectively) suggest that these fragments arise from the OM (Figure 2B and 2C). Indeed, two prominent protein bands of ~ 26 and 32 kDa present in IM are not present in the HcpE-containing membrane fragments and one prominent band at ~ 14 kDa present in OM is also present in our HcpE-containing membrane samples (Figure 2C, bands indicated by *). These membrane fragments also formed readily in the *hcpE* knockout mutant and their properties appeared similar to those of the wild-type strain, with the exceptions that they did not comprise HcpE (as expected) and comprised shorter O-antigens (Figure 2A-C). We therefore tentatively assigned these membrane fragments to outer membrane vesicles (OMVs) since *H. pylori* was previously shown to secrete OMVs (reviewed in (Parker and Keenan, 2012)). OMVs are spherical, bilayered membranous structures which, in *H. pylori*, range from 75 to 150 nm in diameter (Mullaney *et al.*, 2009; Parker and Keenan, 2012). Electron microscopy observation of our samples after uranyl acetate staining confirmed the presence of *bona fide* OMVs (Figure 2D).

192

193 **Modeling of HcpE's structure predicts formation of nine disulfide bonds to stabilize SLR**
194 **domains:** The sequence of HcpE contains nine predicted SLR motifs which should collectively
195 comprise nine disulfide bonds involving 18 cysteine residues (Figure 3) if the structural features
196 demonstrated by crystallography for HcpB/C (Luthy *et al.*, 2002, 2004) also apply to HcpE. An extra
197 cysteine residue is present in the signal peptide of HcpE but is anticipated to be removed from the
198 mature protein after processing of its signal peptide upon secretion through the inner membrane by the
199 Sec machinery.

200 To investigate if the formation of multiple disulfide bonds is also a key feature of HcpE folding,
201 the structure of HcpE was modeled using the SwissProt modeling software. The best fit was obtained
202 with the structure of HcpC as a template (Figure 4, panels A, B) (Luthy *et al.*, 2004). In the obtained
203 model, SLRs 1-3 and 6-9 of HcpE were superimposed to the seven SLRs of HcpC, whereas a stretch of
204 62 amino acids (amino acids 152 to 213) comprising the two central SLR repeats of HcpE (SLRs 4 and
205 5) was left misaligned (Figure 4, panel B). The predicted secondary structure elements of this
206 misaligned stretch of amino acids were for the most part α-helices, as expected if this sequence was
207 part of genuine SLRs. This suggested that the structure of this portion of the protein might not be
208 properly modeled using HcpC. Also, the model showed disulfide bonds between Cys residues of SRLs
209 1-3 and 6-9, as expected, but left the four Cys present in SLRs 4 and 5 in their reduced form, which
210 was unexpected. It is possible that this inconsistent model reflects the fact that HcpE comprises more
211 SLRs than HcpC, preventing correct modeling of some of them.

212 To resolve this issue, HcpE was re-modeled as two separate but overlapping moieties that each
213 comprised less SLRs than HcpC, and each comprised SLRs 4 and 5. Specifically, the N-terminal
214 moiety was modeled using amino acids 1-230, and the C-terminal moiety was modeled with amino
215 acids 143-355. Using each segment for structure modeling, the structure of SRLs 4 and 5 was properly
216 modeled onto that of HcpC, with predicted oxidized Cys residues maintaining the two helices of each

SLR (Figure 4, panel C). The predicted structure of the remainder of the protein remained identical to that predicted with the full-length sequence, i.e. all expected SRLs modeled as the anticipated V-shape two-helix structure interconnected via a disulfide bridge. Alignment of both N and C-terminal segments via their overlapping SLRs using PyMol allowed the production of a reconstituted HcpE model (Figure 4, panel D). In this model, the regular two-helix motif of the SLRs is maintained throughout the structure of HcpE and gives rise to a super helix with a full 360 degree span. Similar results were obtained by modeling the structure of other Hcps (Table I, and supplementary Figure S1).

Structure-based sequence alignment of HcpE validates the 3D model: A structure-based sequence alignment of the nine SLR motifs produced from the reconstituted HcpE structure provided perfect alignment of the Cys residues within these motifs, with seven intervening residues between the two Cys of each SRL motif (Figure 5). Also, this structure-based alignment showed high level of sequence conservation at positions 3 (K), 4 (A), 7 (Y), 8 (F/Y), 10 (K), 11 (A/G), 12 (C), 21 (C), 24 (L), 25 (G), 28 (Y/F) in HcpE. Some of these features, including conservation of aligned cysteines interspersed by seven amino acids, did coincide with the sequence alignment generated from the HcpC structure (Luthy *et al.*, 2004) (Figure 5), although the boundaries of helices differed slightly between HcpE and HcpC. This structure-based sequence alignment validated the global accuracy of the modeled structure for HcpE.

Identification of HP0231 as folding factor for HcpE by affinity blotting: The facts that the predicted structure of HcpE described above contains numerous disulfide bonds in a very precise pattern, that HcpE has a Sec secretion signal to transport it towards the periplasm, and that the Sec machinery only transports unfolded proteins (Natale *et al.*, 2008) altogether suggest that HcpE might interact with periplasmic proteins of the Dsb (DiSulfide Bond) family in the periplasm to acquire its proper structure prior to final secretion. To identify folding factors that interact with the incoming

unfolded and reduced HcpE in the periplasm, we used the "affinity blotting of immobilized substrate" technique. This technique has been used extensively to detect interactions between Type III chaperones and their cargos (Bennett and Hughes, 2000; Bennett *et al.*, 2001; Fraser *et al.*, 1999; Wattiau *et al.*, 1994). Because the interaction between a folding factor and its substrate involves the unfolded substrate (i.e HcpE in our case), HcpE was overexpressed in *E. coli* with an hexa-histidine tag, and purified HcpE-His was blotted onto a PVDF membrane after SDS-PAGE (which reduces and denatures it). A matching Coomassie-stained gel (Supplementary Figure S2) was used to ascertain the position of HcpE on the membrane. Two bands corresponding to HcpE were identified: one was the full-length HcpE-His (~41 kDa with the His-tag) and the other was a ~30 kDa truncated form of HcpE that arises spontaneously from degradation of HcpE as ascertained by anti-HcpE Western blotting (Figure S2). The membrane was incubated with total soluble *H. pylori* proteins so that the membrane-bound reduced and denatured HcpE could interact with folding factors from the cell extract, such as Dsb proteins. The two bands were cut out individually and the interacting partners were identified by mass spectrometry (MS) after trypsic digestion. The procedure was also conducted on a control *H. pylori* protein TsaA expressed with a histidine tag (TsaA-His, migrating at ~27 kDa, Figure S2) and purified in the same conditions as HcpE-His. TsaA served a dual purpose in this experiment. First, TsaA (also known as AhpC) is a typical alkyl hydroperoxide reductase involved in peroxide detoxification via oxidoreduction of its two catalytic cysteines (Poole, 2005). Recycling of AhpCs involves reduction of their oxidized cysteines by cysteine-containing tripeptide glutathione or by thioredoxin or glutaredoxins (Prinz *et al.*, 1997). We therefore expected to obtain hits for a variety of factors involved in thiol oxidoreduction using TsaA, and in this regard TsaA served as a positive control. On the other hand, TsaA also served as a negative control to eliminate background noise and allow selection of hits that would be specific for HcpE and would not simply relate to the presence of exposed hydrophobic domains of the denatured target proteins, to the presence of cysteines or to the presence of a histidine tag.

For each of the full-length and the truncated HcpE proteins and for the TsaA control, several MS hits were obtained for proteins involved in general metabolism, cell maintenance and protein synthesis, which may not represent specific interactions but may rather reflect the high abundance of these proteins (Data not shown). Hits were also obtained for general folding factors such as a peptidyl-prolyl cis/trans isomerase, the DnaK chaperone and the GroES and GroEL chaperonins (Table II). This may reflect the fact that these factors bind hydrophobic domains of proteins that are usually buried in the core of folded proteins and are only exposed in unfolded substrates, as present in our TsaA and HcpE proteins once they are blotted onto the membrane. While obtaining these hits validated our method as an adequate tool to detect interactions with folding factors, these folding factors are not specific for cysteine-containing proteins. We also obtained hits for thioredoxin for all samples (Table II), which further validated the method to detect interactions for cysteine-containing proteins and their redox partners. As explained above, the TsaA / thioredoxin interaction was expected based on physiological processes but the fact that hits for thioredoxin were also obtained with the HcpE samples highlights the non-specific nature of the interaction beyond the targeting of cysteine-containing proteins. Indeed, since HcpE is a periplasmic protein and thioredoxins are cytoplasmic proteins, this *in vitro* interaction likely simply reflects the high efficiency of thioredoxins *in vitro* towards all cysteine-containing proteins (Prinz *et al.*, 1997). Collectively, the lower numbers of hits obtained for the HcpE samples compared with the TsaA sample reflect the lower abundance of HcpE than TsaA on the membrane. This was apparent by SDS-PAGE and Coomassie staining (Figure S2) but also by the recovery of less peptides for the input HcpE (3 peptides only) than for input TsaA (15 peptides). Input HcpE was actually only identified in the full length HcpE band but not in the truncated HcpE band although the presence of HcpE had been ascertained by Western blot. Therefore, lower recovery of peptides could also reflect their different nature and ionization efficiency compared with TsaA-derived peptides.

Once all non-specific hits were eliminated, a hit specific for HcpE became apparent. This hit corresponded to open reading frame HP0231 and was obtained with both forms of HcpE (full length

and truncated) but not with TsaA, suggesting that HP0231 is a specific interacting partner of HcpE (Table II). The hit was based on a single peptide (MQDNLVSVIEK), affording 4% sequence coverage with individual peptide scores of 99.6 and 99.1% for full length and truncated HcpE, respectively. HP0231 corresponds to the DsbG homologue mentioned in the introduction, which we have renamed DsbK in this manuscript based on the functional data described below. Note that the molecular weight of DsbK is 29.5 kDa, similar to that of the *E. coli* DsbG homologue, but it was identified from analysis of the excised full length HcpE-His band that migrated at ~41 kDa, (in addition to being recovered also from the truncated HcpE) and can therefore not represent contaminating *E. coli* DsbG protein carried forward during HcpE purification. Also, the sequence of the identified peptide is not conserved in *E. coli* DsbG but is specific to DsbK.

This interaction between DsbK and HcpE has never been identified before to the best of our knowledge. For example, search of the PIMRider protein/protein interaction database (http://pim.hybrigenics.com/PIMRider/PIMRider-categories/ENTRY-POINTS.html), established based on yeast two-hybrid screening (Rain *et al.*, 2001) yielded potential interactions of DsbK with 8 proteins, but the scores obtained suggest that the interactions may be non specific, none of these were confirmed biochemically and none of these encompassed HcpE. This new and specific interaction highlighted by the affinity blotting method suggests a role of DsbK in assisting the folding of HcpE via formation of disulfide bonds. This was demonstrated via direct *in vitro* biochemical assays and via *in vivo* assays as described below.

DsbK is necessary for the production and secretion of HcpE in *H. pylori*: DsbK was identified as interacting with reduced and denatured HcpE *in vitro*, suggesting that HcpE is a potential substrate for DsbK and that DsbK is an important folding factor for HcpE. However, it is not known whether DsbK is essential for the production and secretion of HcpE in *H. pylori* or if other Dsb proteins may fulfill this role in the absence of DsbK. To test this hypothesis, a knockout mutant was produced by

disrupting the *hp0231* gene (which codes for DsbK) by a kanamycin resistance cassette in strain NCTC11637. The production and secretion of HcpE in the resulting *dsbK* mutant was assessed by anti-HcpE Western blotting of various cellular fractions (Figure 6A) and cell lysis was assessed by measuring the urease activity of these fractions (Figure 6B). In contrast to the wild-type strain, hardly any HcpE could be detected in total cells (~47 times less as per densitometry of the HcpE signal normalize to total protein amount loaded on the gel) or in the cytoplasm of the *dsbK* mutant. The mutant nevertheless produced small amounts of HcpE which could be detected mainly in periplasm-enriched fraction and to a much lower extent into the OMVs. Indeed, the periplasmic to cytoplasmic ratio of HcpE (normalized to total protein amounts in each lane) was higher in the mutant (4.8) than in the wild-type (2.9), and the same trend was observed for the ratio of HcpE present in the periplasm compared with the OMVs (3.5 in the mutant versus 1.9 in the wild-type). The data indicate that in the wild-type strain, HcpE is targeted to the periplasm as predicted and that the small amount of HcpE protein that is produced in the *dsbK* mutant is still properly targeted towards the periplasm but that its export in the OMVs is sub-optimal. The very low amount of HcpE observed in OMVs from the *dsbK* mutant is likely due to a specific effect of DsbK on HcpE folding prior to secretion as opposed to a general pleiotropic effect of this mutant that would interfere with OMV formation as indicated by the normal protein and LPS profiles of the OMV and IM and OM fractions of this mutant (Figure 2). While production of a pure periplasmic fraction devoid of cytoplasmic proteins could not be achieved under any of the conditions tested due to premature lysis of spheroplasts, the finding of HcpE in higher relative abundance in the periplasmic fraction than in the cytoplasmic fraction of the *dsbK* mutant indicates that enrichment in periplasmic proteins was efficiently achieved. This is also confirmed by (i) the higher concentration of HcpE in the periplasmic fraction of the wild-type strain compared with the cytoplasmic fraction, and (ii) the minimal urease activity measured in the periplasmic fraction compared with the high activity measured in the cytoplasmic fraction (Figure 6B). As shown by electron microscopy, the *dsbK* mutant still produced OMVs (Figure 2D). They exhibited normal LPS

and protein patterns (Figure 2A, B), but contained much less HcpE than wild-type OMVs (Figure 2A and 6A).

Altogether, these data demonstrate a direct biological connection between DsbK and the production and secretion of HcpE in *H. pylori* NCTC11637. Similar findings were obtained in strain SS1 whereby production and secretion of HcpE depended on a functional *dsbK* gene (Supplementary Figure S3).

The interaction between insoluble HcpE and DsbK results in solubilization of HcpE: We showed above that HcpE interacts with DsbK using affinity blotting of immobilized HcpE and that DsbK is important for the production and secretion of HcpE in *H. pylori*. Considering the potential role of DsbK in disulfide bond formation and the requirement for an organized array of disulfide bonds in the structure of HcpE, we hypothesized that the interaction between HcpE and DsbK likely results in the formation of proper disulfide bonds in HcpE to assist its folding *in vivo*. *In vitro*, the DsbK-mediated formation of disulfide bonds in misfolded (and therefore insoluble) HcpE is anticipated to result in its solubilization.

Like its HcpA and HcpC counterpart, HcpE tends to be expressed in *E. coli* in an insoluble form at 37^{o}C (Luthy *et al.*, 2004; Mittl *et al.*, 2000) (Figure 7). Induction at lower temperatiure did not increase solubility. However, co-expression of HcpE and DsbK together from the same vector (but nevertheless as independent proteins) resulted in enhanced production of soluble HcpE when induction was performed at low temperature (Figure 7). This indicates that the endogenous *E. coli* Dsb proteins are not able to assist the folding of HcpE.

The insoluble HcpE fraction recovered after elimination of soluble proteins by centrifugation comprised the typical ~41 and 30 kDa bands (on 12% SDS-PAGE gels) corresponding to HcpE (full length and C-terminal truncation as described above) as indicated by reactivity with anti-HcpE antibodies. Using more resolutive 16% SDS-PAGE gels the ~41 kDa band could be resolved further in

two bands that both reacted with the anti-HcpE antibodies (Figure 8). The observed size difference of ~ 3 kDa suggests that the fastest migrating band corresponded to processed (i.e. mature) HcpE whose signal peptide of 2.7 kDa had been removed, while the band of slightly higher molecular weight corresponded to un-processed HcpE that still had its signal peptide. Since signal peptide removal only occurs upon entry in the periplasm, this latter band corresponds to HcpE that has never exited the cytoplasm and has not been exposed to the oxidative environment of the periplasm or to any Dsb protein. It is therefore a prime substrate for DsbK-mediated disulfide bond formation. The insoluble protein suspension was incubated with increasing concentrations of DsbK that had been over-expressed in *E. coli* with a Flag tag (~ 31 kDa total size) and enriched by anion exchange chromatography. Control experiments were performed with anion exchange fractions eluting at the same salt concentrations as DsbK but that were obtained from *E. coli* (of the same background) that did not express DsbK. At the end of the incubation period, the reaction was spun down to pellet the remaining insoluble HcpE, and the reaction supernatant potentially containing solubilized HcpE was analyzed by anti-HcpE Western blotting. We observed that recovery of un-processed HcpE occurred exclusively in the presence of DsbK and that addition of increasing amounts of DsbK allowed its recovery in increasing amounts. In addition to being dose-dependent, the effect of DsbK was time-dependent, as full recovery of un-processed HcpE in the soluble fraction could be obtained with a lower dose of DsbK if the incubation lasted longer. In contrast, the vast majority of processed HcpE present in the input sample was recovered in the supernatant even in the absence of DsbK and addition of DsbK to the reaction did not have any effect on recovery of processed HcpE (Figure 8). This indicates that its prior passage in the periplasm and/or the removal of the signal peptide (which removes 1 cysteine that could otherwise interfere with formation of the organized array of disulfides needed in mature HcpE) is sufficient for this protein to continue folding on its own in the redox buffer conditions used in this assay. Overall, these data demonstrate that the interaction between DsbK and un-processed and unfolded HcpE results in HcpE solubilization.

DsbK has Dsb activity: The experiments above highlight HcpE as a substrate for DsbK and strongly suggest a role for DsbK in assisting disulfide bond formation in HcpE prior to secretion. This is consistent with the fact that DsbK is a putative DsbG protein potentially involved in the isomerization of non native disulfide bonds but its precise biochemical function (role in disulfide bond formation and DsbG vs DsbA type of activity) is still up for debate (Roszczenko *et al.*, 2012; Yoon *et al.*, 2011). DsbK has a predicted Sec signal peptide (Kim *et al.*, 2002) that should support its transfer into the periplasm where it could carry out its Dsb function. However, DsbK is also secreted (Kim *et al.*, 2002) and is a strong antigen (Haas *et al.*, 2002), which is not expected for a genuine Dsb protein. Therefore we investigated if DsbK has Dsb activity using lysozyme as a substrate. We resorted to using this surrogate substrate since the natural substrate of DsbK, HcpE, has no known enzymatic activity that could provide a read out for DsbK activity. In contrast, lysozyme hydrolyses peptidoglycan readily and its folding and stability rely on four disulfide bonds (Eyles *et al.*, 1994; Harata, 1994), which in turn influences its catalytic efficiency. Therefore, inactive denatured and reduced lysozyme was incubated with recombinant DsbK and regeneration of active lysozyme via the Dsb activity of DsbK was monitored spectrophotometrically (OD_{650nm}) by recording the ability of lysozyme to lyse micrococcus cells as described previously (Puig and Gilbert, 1994). Control experiments were performed with *E. coli* DsbG and DsbA proteins which, like DsbK had been overexpressed in *E. coli* with a hexahistidine tag and were purified to homogeneity by nickel affinity chromatography.

As shown on Figure 9, in the absence of lysozyme, the micrococcus cells aggregated slightly, which led to a slight increase in OD_{650nm}. When denatured and reduced lysozyme was added in the absence of any Dsb protein, a slow and rather linear decrease of OD_{650nm} was observed (Figure 9, all panels). This indicated low levels of micrococcus lysis which were probably due to spontaneous refolding of the lysozyme. However, when the denatured and reduced lysozyme had been incubated with either DsbG (Panel A), DsbA (panel B), or DsbK (Panel C), faster and enhanced lysis of

micrococcus cells was observed, with an exponential shape indicative of enzymatic reaction. This indicated that, like DsbA and DsbG, DsbK could assist the regeneration of essential disulfide bonds in lysozyme and therefore has Dsb activity.

In this assay, the efficiency of refolding depends on the original oxidation status of the enzyme preparation used and requires optimization of the ratio of oxidized and reduced glutathione to provide the proper redox balance to support regeneration of the Dsb protein tested. The data presented above were obtained using common conditions to provide a direct comparison of the three proteins (DsbK, DsbG and DsbA). They show a general role of DsbK in disulfide bond formation but yield an overall weak activity for the three proteins compared with the rather high level of spontaneous refolding. Further optimization of the assay conditions for DsbK reduced the amount of spontaneous refolding while allowing for very efficient lysozyme refolding upon addition of DsbK, with lytic activity levels very close to those observed with native lysozyme (Panel D). In conclusion, this assay establishes that DsbK has Dsb activity but does not allow discrimination between a DsbA- and a DsbG- type of activity.

DsbK behaves like DsbA when over-expressed in *E. coli* under optimal growth conditions: We surmised that over-expressing an oxidase like DsbA should enhance the oxidative nature of the periplasm and enhance the proportion of misfolded proteins via incorrect disulfide bridge formation that endogenous levels of isomerases may not be able to cope with. This would likely impair bacterial growth. In contrast, over-expressing an isomerase like DsbG would have little or no impact. Therefore, to discriminate between a DsbA- or DsbG-type of activity for DsbK, we investigated the effect of over-expressing DsbK or control DsbA and DsbG proteins in *E. coli*. All three proteins were cloned with a C-terminal His tag for over-expression (independently) in *E. coli* BL21(DE3)pLys. All strains grew equally well in the absence of induction as seen by spot plating serial dilutions of all cultures (Figure

10A, no induction and no DTT panel). After induction by IPTG for 3 h, all proteins were expressed at levels detectable both by Ponceau S red staining and anti-Histidine tag Western blotting (Figure 10C).

A preliminary experiment performed by spot plating the pre-induced cultures on agar containing IPTG indicated high toxicity of continuous expression of all proteins (Figure S4). Therefore, all further experiments were conducted by spot-platting the pre-induced cultures on agar devoid of IPTG (pre-induction only). In that case, a toxic effect was still observed for DsbK and DsbA but not for DsbG or for an irrelevant control protein (GmD, expressed at very low levels) (Figure 10A). Anti-His Western blot analysis of the cells recovered from the plates after 16h incubation indicated that protein expression had ceased (as expected because of the lack of IPTG) and that all pre-induced proteins had been turned over as no traces of DsbA, DsbG or DsbK could be detected (Figure S5A and B). This indicates that the toxic effect observed for DsbA and DsbK was mediated by the proteins produced during the pre-induction stage and that only cells that did not express the proteins or had eliminated them could survive. Overall DsbK and DsbA behaved similarly in this assay, having a strong toxic effect while DsbG did not.

The DsbA-like behavior of DsbK in *E. coli* is exacerbated under reductive stress: Because *E. coli dsbA* mutants are sensitive to dithiothreitol (DTT) (Bardwell *et al.*, 1991; Kamitani *et al.*, 1992; Roszczenko *et al.*, 2012), the oxidase DsbA is anticipated to be necessary to form disulfide bonds during reductive stress. In such context, few spontaneous bonds would form, and the activity of bond-correcting DsbG would not be important. Hence, investigating the effect of DsbK on the ability of *E. coli* to cope with reductive stress should further discriminate between DsbA or DsbG activity for DsbK.

The cultures from above were therefore also spot-plated on agar containing DTT. No bacteria could be recovered for any of the non-induced strains in the presence of 10 mM DTT but lower concentrations of 5 and 7.5 mM had no noticeable effects (Figure 10A), suggesting that endogenous Dsb proteins allow the bacteria to cope with these lower concentrations of DTT. Unexpectedly, pre-

466 expressing DsbA or DsbK not only did not protect against DTT at any of the concentrations tested but
467 actually severely inhibited bacterial growth so that the toxic effect of pre-expression was exacerbated
468 compared with the "no DTT" control and hardly any cells were recovered. In contrast, only a minor
469 deleterious effect of DTT was observed on DsbG-expressing cells: fewer cells were recovered on DTT-
470 containing plates than on "no DTT" plates but the decrease was similar to that observed with the
471 control protein that was expressed at very low level. The reason why the presence of DsbA or DsbK is
472 more toxic in the presence of DTT than in normal redox conditions is unclear at this stage but this
473 assay nevertheless demonstrates a DsbA-like behavior of DsbK, distinct from the DsbG behavior.
474
475 **The DsbA-like toxic effect of DsbK in *E. coli* is bacteriostatic:** Similar results were obtained when
476 the expression assays were performed in broth with continuous spectrophotometric monitoring of
477 growth. The energetic cost of protein expression combined with the toxic effects highlighted in the
478 plate assay resulted in a longer lag phase for pre-induced cultures but the same culture density was
479 reached at stationary phase for all strains and the growth rate was the same as in the absence of pre-
480 induction (Figure 10B). The lengthening of the lag phase was of lower extent for DsbG (~1h)
481 compared with DsbA (4h) and DsbK (3h) although all proteins were initially expressed at similar levels
482 in the cells used as inoculum for the growth curves (Figure S5C). All pre-induced proteins had been
483 eliminated 6h after inoculation (Figure S5D), which likely explains that all strains grew at the same
484 rates afterwards.
485 Addition of DTT to the growth media further lengthened the lag phase in all strains (pre-induced or
486 not) and decreased the cell density reached in stationary phase compared with the "no DTT" control.
487 Comparison of the lag phase length for each strain with or without pre-induction under the same DTT
488 concentration also discriminates between DsbG- and DsbA-types of activities for DsbK, with hardly
489 any extra deleterious effect upon DsbG expression while expression of DsbA or DsbK greatly
490 lengthened the lag phase. All pre-induced proteins had been eliminated in the cells tested after

exponential growth in the presence of DTT (Figure S5E) which likely allowed all cultures to reach the same optical density.

Overall, the two types of DTT-exposure assays (plate- and broth-based) support a DsbA-like behavior of DsbK when expressed in *E. coli* rather than a DsbG-like activity. Furthermore, the broth-based assay indicates that the DsbA and DsbK toxic effects are bacteriostatic rather than bactericidal.

Inactivation of *dsbK* increases sensitivity of *H. pylori* to atmospheric oxygen and impairs resistance to oxido-reductive stress: Beyond its role in HcpE secretion, the physiological role of DsbK for *H. pylori* is unknown. DsbK is not necessary for survival under the microaerobic conditions used to obtain the *dsbK* knockout mutant and is also not necessary for microaerobic growth in broth since similar optical densities were attained for the *dsbK* mutant and the wild-type strain (Figure 11A). However, spot plating of these cultures for cfu determination revealed a statistically significant ~0.5 to 1 log reduction of viability for the *dsbK* mutant (Figure 11B). This likely represents an enhanced sensitivity of the mutant to atmospheric oxygen that the cells were exposed to (for ~ 30 min) during spot plating. Longer exposure (tested up to 1h30) did not decrease viability further, indicating that compensatory mechanisms may be triggered to handle the oxidative stress. Alternatively, this may indicate that the viability of the *dsbK* mutant had already decreased during microaerobic growth before spot-plating.

The exacerbated sensitivity of the *dsbK* mutant to oxidative stress was further demonstrated by exposing the wild-type and *dsbK* mutant to various concentrations of H_2O_2 for 30 min (under microaerobic conditions) before spot plating (Figure 11C, lower panels, quantitation Figure 11E). Hardly any growth was observed for the *dsbK* mutant upon exposure to 100 mM H_2O_2 and growth was totally suppressed with 125 mM H_2O_2, while wild-type bacteria were readily recovered. We also tested any effect on resistance to reductive stress by spot plating the different strains on plates containing DTT (Figure 11C, upper panels, quantitation Figure 11E). While none of the strains was sensitive to

DTT up to 8 mM, all exhibited sensitivity to 12 mM DTT, with much enhanced sensitivity of the *dsbK* mutant compared with the wild-type strain. All effects described were specific for *dsbK* as none were seen for the *hcpE* mutant with DTT and only very small effects were seen with H_2O_2. The effects of H_2O_2 and DTT on the *dsbK* mutant could be complemented *in trans* by chromosomal integration of a functional *dsbK* gene (Figure 11D, quantitation Figure 11E).

Overall, these data show that, despite the presence of other Dsb homologues in *H. pylori*, DsbK fulfills at least two important functions in *H. pylori*: it controls the secretion of proteins (including HcpE) under optimal microaerobic conditions and also controls bacterial viability via its role in maintaining redox homeostasis against exposure to environmental redox factors.

Discussion:

Specific activity and function of DsbK: The mechanism of disulfide bond formation in *H. pylori* is still poorly understood and two recent studies on DsbK have yielded contradictory results (Roszczenko *et al.*, 2012; Yoon *et al.*, 2011). This mirrors the difficulties encountered to elucidate the activity of the *E. coli* DsbG (Andersen *et al.*, 1997; Bessette *et al.*, 1999; Depuydt *et al.*, 2009; Missiakas *et al.*, 1993; Shao *et al.*, 2000; van Straaten *et al.*, 1998). Our work provides functional evidence that DsbK has Dsb activity on a surrogate substrate, and suggests a DsbA-like activity (oxidase) rather than a DsbG-like activity (isomerase) when expressed in *E. coli*. Although our finding of DsbA-type activity for DsbK was unexpected in view of its homologies to *E. coli* DsbG (Yoon *et al.*, 2011), it is in agreement with functional data obtained using insulin as a substrate (Roszczenko *et al.*, 2012).

Our *E. coli*-based DTT sensitivity assays relied on the premise that an oxidase (DsbA type) would be more important under reducing stress than an isomerase (DsbG type), so that expression of DsbA was anticipated to provide relief against DTT stress while expression of DsbG would have little to no effect. Accordingly, no toxicity or benefit of overexpression of DsbG was observed in the presence or absence of DTT, but unexpectedly, expression of DsbA or DsbK was toxic in two types of assays under

various concentrations of reducing agent. While we can not explain this toxicity at this stage, both assays clearly distinguish between a DsbA versus DsbG activity for DsbK in *E. coli*.

The behavior differences between the *H. pylori dsbK* mutant and the *E. coli dsbG* mutant also suggest that DsbK and DsbG may not have the same activity and biological role. Indeed, the *E. coli dsbG* mutation is conditionally lethal, and mutants can not be recovered unless an oxidant or cystine is added to the growth medium (Andersen *et al.*, 1997). In contrast, we and others could readily obtain the *dsbK* knockout mutant in a variety of *H. pylori* strains in the absence of any additives (this study for strains SS1 and NCTC 11167, and (Roszczenko *et al.*, 2012) for strain N6), and the bacteria were grown under microaerobic (i.e. less oxidative) conditions. We demonstrated that this mutant was sensitive to oxidative stress, clearly highlighting physiological differences in the role of *H. pylori* DsbK and *E. coli* DsbG. To our surprise, the sensitivity to oxidative stress could not be alleviated by adding a reducing agent to the medium as the mutant also showed sensitivity to DTT. These data indicate that DsbK is likely involved in both the isomerisation and the oxidative pathways in *H. pylori*, thereby fulfilling both DsbA and DsbG activities. This reconciles the biochemical and structural data supportive of DsbG activity with its DsbA-like behavior in *E. coli*.

Furthermore, most HcpE produced in *E. coli* was insoluble, no matter what host (BL21(DE3), BL21(DE3)pLys, ER2526), expression media or temperature are used. Only co-expression of HcpE with DsbK increased the yield of soluble HcpE (Figure 7). Beyond further supporting the role of DsbK in the folding of HcpE, this also points out that despite homologies to DsbG and despite a DsbA-like behavior, DsbK has features not exhibited by endogenous *E. coli* DsbG or DsbA which fail at processing HcpE efficiently. This could also suggest that the complement of endogenous *E. coli* Dsb proteins is not sufficient to handle the large amount of HcpE produced upon over-expression.

Biological linkage between HcpE and DsbK: This work is the first to identify a biological substrate for DsbK. To date, only surrogate substrates have been used to demonstrate the activity of DsbG

566 proteins (Andersen *et al.*, 1997; Roszczenko *et al.*, 2012; Shao *et al.*, 2000). Even in *E. coli*, methods
567 that identified substrates for other Dsb proteins failed at identifying DsbG substrates (Depuydt *et al.*,
568 2009; Hiniker and Bardwell, 2004). Recently, a DsbG CXXA mutant was used to trap periplasmic L,D-
569 transpeptidases as DsbG substrates, although each only contains a single cysteine and thus does not
570 require disulfide bond formation (Depuydt *et al.*, 2009). In *H. pylori*, two hybrid assays did not identify
571 *bona fide* interacting partners for DsbK (Rain *et al.*, 2001) and *in vitro* activity of DsbK on HP0518
572 was demonstrated based on the premise that HP0518 contains the same L,D-transpeptidase domain as
573 found in *E. coli* DsbG substrates, but no biological linkage between HP0518 and DsbK was established
574 (Yoon *et al.*, 2011). Therefore, the DsbK /HcpE interaction described in this work that was ascertained
575 by affinity blotting, direct biochemical data and knockout mutagenesis is the first discovery of a
576 biologically relevant substrate for DsbK. This is reinforced by the facts that (i) DsbK (a.k.a. HP0231) is
577 encoded in proximity to HcpE (a.k.a. HP0235) on the bacterial chromosome, although both are
578 encoded on divergent DNA strands, and (ii) that there is a feedback regulatory loop whereby the total
579 amount of HcpE produced is drastically reduced in the *dsbK* knockout mutant, which could occur at the
580 transcriptional level or by enhanced degradation of misfolded HcpE. Our data do not exclude that other
581 proteins such as other Hcp proteins could also serve as substrate for DsbK.
582
583 **DsbK -assisted folding of HcpE may also be important for its OMV-mediated secretion:** A portion
584 of HcpE is secreted via OMVs in a DsbK-dependent manner. The formation of OMVs by *H. pylori* is
585 well documented with functional implications for biofilm formation, activation of phagocytic and
586 gastric cells, and potential delivery of toxins to gastric cells (reviewed in (Parker and Keenan, 2012)).
587 Two proteomics studies investigated the general protein composition of OMVs, reporting the presence
588 of HcpC, D, E, F and G, although not all proteins were actually identified as Hcps (Mullaney *et al.*,
589 2009; Olofsson *et al.*, 2010). The functional significance of this OMV-mediated secretion of HcpE will
590 be investigated as soon as the biological activity of HcpE has been elucidated.

The *dsbK* mutant OMVs appeared similar to wild-type OMVs by electron microscopy and by its total protein composition, except for its lower HcpE content. We can not exclude that the export of other Hcps to the OMVs is also affected but could not check this for lack of appropriate antibodies. The data suggest that DsbK-assisted folding of HcpE is important for OMV-mediated secretion of HcpE. Beyond testing the (unknown) biological activity of these HcpE-containing OMVs, there is no way to establish that the enclosed HcpE is actually folded.

Finally, we noted association of urease with the OMVs by measuring urease activity (Figure 6). Whether urease is released extracellularly via cell lysis or active secretion is controversial (Marcus and Scott, 2001; Vanet and Labigne, 1998) and conflicting data were reported as to the presence of urease within OMVs or as contaminants of OMVs (Mullaney *et al.*, 2009; Olofsson *et al.*, 2010; Parker and Keenan, 2012). The urease activity measured could stem from urease oligomers co-pelleted with the OMVs upon ultracentrifugation, notwithstanding the original mode of release of urease, since EM revealed structures reminiscent of urease doughnut-like oligomers (Austin *et al.*, 1991; Hawtin *et al.*, 1990) interspersed with the OMVs. Thus, low levels of lysis not detected in bulk supernatant could be detected in OMV fractions after concentration of urease by oligomerisation and ultracentrifugation.

Implications for the DsbK /HcpE interaction and mechanism of action of DsbK: Our refolding studies indicated that un-processed HcpE (i.e. with signal peptide) was a substrate for DsbK while the processed form was not and could fold by itself in the assay conditions. This indicates that its prior passage in the periplasm and concomitant removal of its signal peptide are beneficial to initiate folding. The signal peptide comprises a cysteine that can potentially shift the pattern of disulfide bond formation (signal peptide to SLR1, SLR1 to SLR2 etc instead of intra-SLR bonds) if folding occurs spontaneously. Our data suggest that assistance from DsbK may restore the proper pattern of disulfide bonds in the presence of this extra Cys residue, and/or that DsbK initiates the oxidation step that failed to occur for the un-processed HcpE that was only exposed to the relatively reducing cytoplasm.

This work does not exclude that additional folding factors may be important for a productive HcpE / DsbK interaction. Our disulfide bond forming assay ensures regeneration of the redox status of DsbK by addition of redox compounds. *In vivo*, interaction with a second Dsb protein such as DsbI (Roszczenko *et al.*, 2012) likely fulfills this role. DsbI was not identified in our affinity assay likely because we used soluble extracts while DsbI is membrane-bound, a feature necessary to benefit from the membrane electron transport chain. Lacking DsbI in our system may have prevented regeneration of DsbK, thereby locking it onto its substrate and allowing its permanent capture.

Overall, this work provides novel insights into disulfide bond formation in *H. pylori*, and specifically about the role of DsbK in *H. pylori*'s physiology. It provides biochemical functional data for DsbK showing a DsbA-type of activity and mutagenesis data showing both DsbA- and DsbG-types of activity in *H. pylori*. This work also identifies the first endogenous substrate for DsbK as a member of the Hcp family that is likely linked to bacterial pathogenesis. Further efforts are now underway to determine the specific role of DsbK in bacterial virulence, to identify potential additional substrates and exploit DsbK and disulfide bond formation for the development of new therapeutics against *H. pylori*.

Experimental procedures:

Bacterial strains and growth conditions: *H. pylori* NCTC11637, SS1 or 26695 cells were grown under microaerobic conditions of 5% O_2, 10% CO_2, and 85% N_2 for 48 hours on Brain Heart Infusion / yeast extract (BHI-YE) or Brucella agar plates containing 10% fetal bovine serum or on Columbia agar plates containing 10% blood. All plates were supplemented with 0.05 µg/ml sodium pyruvate and background antibiotics: trimethoprim (5 µg/ml), vancomycin (10 µg/ml), and amphotericin B (5 µg/ml). The media was further supplemented with kanamycin (5 µg/ml) to select for the *hcpE::kan* and *hp0231::kan* knockout mutants and chloramphenicol (8 µg/ml) to select for the complemented strain. Unless stated otherwise, growth of *E. coli* was done at 37˚C, in Luria-Bertani media supplemented with

chloramphenicol (34 μg/mL), kanamycin (30 μg/ml), or ampicillin (100 μg/ml) as required for selection of expression plasmids.

Cloning of *hcpE*, *hp0231*, *tsaA* and *gmd* genes into the pET system: All primers used in this work are listed in Table III. All standard molecular techniques were as described in (Sambrook *et al.*, 1989). All *H. pylori* genes were PCR amplified from chromosomal DNA of *H. pylori* strain NCTC11637 unless otherwise stated. The *tsaA* gene was amplified with primers HP1563P7 and HP1563P2. The PCR product was digested with AfIII and BamHI and cloned into the pET23 derivative (Newton and Mangroo, 1999) with an N-terminal histidine tag yielding pET23-His-TsaA. The *hp0235* gene coding for HcpE was amplified with primers HP0235P1 and HP0235P2. The PCR product was cloned into the BamHI/EcoRI sites of pUC18 to create pUC18-*hp0235*. The *hp0235* gene was PCR amplified from pUC18-*hp0235* using primers HP0235P8 and HP0235P9 and was sub-cloned into the NotI and NdeI sites of the pET30a plasmid (Novagen) to create pET30a-HcpE-His that codes for C-terminally histidine tagged HcpE. The *hp0231* gene was amplified with primers HP0231P1 and HP0231P2. The PCR product and the pET30a vector were cut with NdeI and BamHI and ligated together to yield pET30a-HP0231-Flag that codes for C-terminally flag tagged DsbK. The *cj1319* gene (coding for GmD) was amplified from *Campylobacter jejuni* strain NCTC11168 using primers Cj1319P9 and Cj1319P10 and cloned into the NdeI and XhoI sites of the pET30a vector to yield pET30a-GmD-His. All constructs were transformed into *E. coli* DH5α cells with selection with ampicillin or kanamycin when appropriate. Positive transformants were verified by restriction enzyme digestion and DNA sequencing (Robarts Research Institute at the University of Western Ontario).

Construction of a duet vector co-expressing DsbK-Flag and HcpE-His: To subclone HcpE-His into the pET30-HP0231-Flag construct generated above, HcpE-His was PCR-amplified from pET30a-HcpE-His with primers T7ProX and CtermHis (Table III) which carry XbaI and BamHI sites,

respectively. The pET30a-HP0231-Flag construct was cut with NheI and BamHI and was ligated with the cut HcpE-His PCR product to yield pET30a-HP0231-Flag-HcpE-His. In this construct, both proteins are co-expressed from the T7 promoter as independent translational units. This construct was used to enhance expression of soluble HcpE-His in *E. coli* BL21(DE3)pLys.

Cloning HP0231-Flag-His in the pET vector: A cleavable C-terminal histidine tag was introduced downstream of the Flag tag in the pET30a-HP0231-Flag construct to allow expression of DsbK-Flag-His. For this purpose, inverse PCR was conducted on the pET30a-HP0231-Flag construct described above using primer HP0231P3 and HP0231P4. Primer HP0231P4 primed in the C-terminal histidine-tag coding DNA of the pET30 vector while primer HP0231P3 primed in the FlaG tag and introduced a TEV protease cleavage site (ENLYFQS, (Kapust *et al.*, 2001)) and a small linker (GS) between the Flag tag and the His tag on the final construct. Both primers had a 5' BamHI site. The PCR product was cut with BamHI before ligation with T4 ligase.

Construction of *E. coli* DsbA- and DsbG-Flag-His expression clones: The *E. coli dsbA* and *dsbG* genes were PCR amplified from strain DH5α using primers DsbAEcP1/P2 and DsbGEcP1/P2, respectively. The PCR products were cut with NdeI and BamHI and were ligated with the gel-purified vector portion of the NdeI and BamHI cut pET30a-HP0231-Flag-His. This yielded pET30a-DsbA-Flag-His and pET30a-DsbG-Flag-His.

Over-expression, and purification of soluble proteins using nickel chelation chromatography: Protein expression was done in *E. coli* BL21(DE3)pLysS (Novagen). The cultures were grown at 37˚C in 1l of LB until they reached an OD_{600nm} of 0.6. For optimal expression of HcpE, cultures were equilibrated to room temperature for 1 hr before induction with 0.15 mM Isopropyl β-D-1-thiogalactopyranoside (IPTG) over night at room temparature. For all others, induction was carried at

690 37°C for 3 h. The cells were harvested by centrifugation at 2,057 *g* for 30 minutes at 4˚C and stored at -
691 20˚C until needed. For purification of the over-expressed proteins the cell pellet was re-suspended in 30
692 ml cold binding buffer (5 mM imidazole, 0.5 M NaCl, 20 mM Tris pH 8.3) supplemented with 1 ml of
693 1M protease inhibitor cocktail (PIC; Invitrogen). The cells were lysed by mechanical disruption (4
694 passages through French press at 15,000 psi in the presence of 150 µg/ml lysozyme or 2 passages in
695 cell disruptor (Constant Systems LTD IS6/40/BA/AA model) at 25,000 psi, no lysozyme added). Cell
696 debris and insoluble proteins were removed by centrifugation at 12,000 *g* for 30 minutes at 4˚C, and
697 membranes were removed by ultracentrifugation (Beckman) at 100,000 *g* for 1 hr. The supernatant was
698 filtered through 0.8 µm and 0.45 µm pore size filters (Millipore Millex-HV) and used for protein
699 purification. The histidine-tagged proteins were purified using a POROS 1.6 mL column (Applied
700 Biosciences) as described before (Butty *et al.*, 2009). The pH of all buffers was adjusted to pH 8.3 for
701 HcpE and TsaA, and pH 7.5 for DsbK and *E. coli* DsbG and DsbA. Fractions containing pure proteins
702 were dialyzed overnight in 50 mM ammonium bicarbonate buffer pH 8.3 or 7.5 as appropriate using a
703 molecular weight cutoff of 3.5 kDa. Protein concentrations were determined by Bradford assay
704 (Biorad). The fractions were stored in the presence of 25% glycerol at -20°C.
705
706 **Expression and enrichment of DsbK-Flag by anion exchange chromatography:** DsbK-Flag (no his
707 tag) was over-expressed from the pET30a-HP0231-Flag construct in BL21(DE3)pLys cells via
708 induction with 0.1 mM IPTG at 37˚C O/N. Cells from 1 l of culture were re-suspended in 30 ml of
709 protein loading buffer (20 mM Tris pH 7.5, 0.5 mM NaCl) containing lysozyme at 150 µg/ml. They
710 were processed as described above and the soluble proteins were separated by anion exchange
711 chromatography using a 1.04 ml AcroSep™ Q Ceramic HyperD F column (PALL Life Sciences).
712 Bound proteins were eluted using a NaCl concentration gradient (from 50 mM to 0.5 M) in 20 mM Tris
713 pH 7.5 buffer. Fractions were analyzed via SDS-PAGE and Western blotting with anti-Flag primary

antibody and goat-anti-mouse secondary antibodies. The protein concentration was determined by Bradford assay (Biorad).

Construction of the *H. pylori hcpE* and *dsbK* knockout mutants: Inverse PCR amplification of *hp0235* from pUC18-*hp0235* was performed with primers HP0235P4 and HP0235P5 (Table III) using Expand Long-Range template polymerase (Roche). The kanamycin cassette was inverse amplified from the pHel3 vector (Heuermann and Haas, 1998) using Aph3P1 and Aph3P2. After digestion with *Cla*I and *Bgl*II, the PCR products were ligated together to create plasmid *php0235::kan.* The *hp0231* gene was sub-cloned from the pET-HP0231-Flag construct into the BamHI and EcoRI sites of pUC18 by amplification with primers HP0231P5 and HP0231P2. Inverse PCR was then performed with primers HP0231P6 and HP0231P7 which introduce ClaI and KpnI sites. The kanamycin resistance cassette was amplified from pHel3 with Aph3P2 and Aph3P4 and both products were cut with ClaI and KpnI and ligated together to produce pUC-*hp0231::kan*. The plasmids were transformed into *E. coli* DH5α cells with selection on ampicillin and kanamycin. To generate the *H. pylori* knockout mutants, the constructs were transformed into *H. pylori* NCTC11637 or SS1 following previously described procedures (Hopf *et al.*, 2011; Merkx-Jacques *et al.*, 2004). The mutants were selected with 4 μg/ml kanamycin. Transformants were analyzed for proper gene integration by PCR using genomic DNA isolated with the InstaGene Matrix (BioRad). The primer pairs used were HP0235P1/P2, P2/P10 and P5/P10 for the *hcpE* mutant and HP0231P1/P2 and HP0230P2/HP0232P3 for the *dsbK* mutant.

Complementation of the *H. pylori hp0231* knockout mutant: The *hp0231* gene and 500 bp upstream and downstream were amplified from *H. pylori* 26695 chromosomal DNA with primers 231Comp1 and 231Comp2. The PCR product was cloned into the PstI and EcoRI sites of the pUC18 vector to obtain pHP231op. The sequenced plasmid was then used as a template in an inverse PCR reaction using primers 231Comp3 and 231Comp4 that prime at the end of the *hp0231* gene and allow incorporation of

a N-terminal histidine tag. Separately, a chloramphenicol resistance cassette was amplified from pHel2 vector (Heuermann and Haas, 1998) using CatHelP1 and CatHelP2. After digestion of both PCR products with XbaI and BamHI, they were ligated together and transformed into *E. coli* DH5α to obtain plasmid pHP231opCAT. This plasmid was methylated *in vitro* with *H. pylori* NCTC11637 cell free extracts and S-adenosylmethionine (Donahue *et al.*, 2000) and was introduced in the *H. pylori* *dsbK* mutant by natural transformation with selection with chloramphenicol (Ge and Taylor, 1997). Integration of the complementing gene was ascertained by PCR.

Production and screening of anti-HcpE antibodies: HcpE-His was over-expressed from the pET30a-HcpE-His construct as described above. As HcpE was expressed mainly in an insoluble form, it was purified by metal chelation in the presence of 6M guanidine-HCl. Eluted fractions were dialyzed in 50 mM ammonium bicarbonate pH 8.3, diluted 1/1 (vol/vol) with 1.7 % saline and the mixture was used to immunize 2 New Zealand white rabbits after a further 1:1 (vol/vol) dilution with Freund's adjuvant (Sigma) and filter sterilization. On day 1, the rabbits were immunized with 1 mL of protein preparation containing 500 µg HcpE prepared with complete adjuvant. The rabbits were boosted on days 14 and 28 with 150 µg of HcpE (comprised in 1 ml with incomplete adjuvant). Blood was collected prior to each injection. The final blood harvest was performed on day 36. Animal care, inoculations and blood collection were performed by the Animal Care and Veterinary Services at the University of Western Ontario according to the approved protocol 2007-103 (from Dr. I. Welch). The blood was allowed to coagulate for 1 h at room temperature and overnight at 4˚C. The serum was obtained via centrifugation at 12 000 *g* for 10 minutes and was stored at -20˚C.

The specificity of the antibody was determined by Western blotting on total cell extracts from *E. coli* over-expressing HcpE-His or total *H. pylori* extracts. Detection was done with goat anti-rabbit IgG secondary antibody conjugated to Alexa fluorophor detected at 800 nm on a Licor Odyssey instrument. To enhance the specificity of the antibody, aliquots of serum were absorbed against *E. coli*

764 BL21(DE3)pLysS for detection of HcpE in our *E. coli* expression system, or against the *hcpE::kan*
765 mutant to enhance detection of HcpE in *H. pylori*.
766
767 **Analysis of the *H. pylori* secretome to assess HcpE secretion:** Wild-type and *hcpE* mutant *H. pylori*
768 strains were grown on BHI-YE plates with background and selective antibiotics for 48 hrs. The cells
769 were harvested and inoculated at OD_{600nm} of 0.2 in 30 ml of brucella broth supplemented with 1% β-
770 cyclodextrin (Marchini *et al.*, 1995) and the required antibiotics. The cultures were incubated for 12,
771 16, or 20 h at 37˚C under microaerobic conditions with gentle agitation. At each time point, aliquots of
772 culture were set aside for OD_{600nm} readings and quantification of cell lysis by the phenol red assay
773 (Clyne *et al.*, 1995; Merkx-Jacques *et al.*, 2004). The remaining cells were pelletted via centrifugation
774 at 2,057 *g* for 30 minutes at 4˚C. Proteins recovered in the supernatants were concentrated by
775 trichloroacetic acid (TCA) precipitation. Briefly summarized, 10% ice-cold TCA was added to the
776 supernatant in a 1:1 (vol/vol) ratio. After 15 minutes of incubation on ice, the samples were centrifuged
777 at 16,000 *g* for 15 minutes at 4˚C, the supernatant was removed, and the precipitated proteins were
778 washed in acetone. The samples were centrifuged again for 5 minutes at 16,000 *g* and pellets were air
779 dried at room temperature. The proteins were separated by SDS-PAGE (15%) and detected by Western
780 blotting with anti-HcpE primary antibodies and goat anti-rabbit IgG secondary antibody.
781
782 **OMV preparation:** The bacteria were inoculated in cyclodextrin-containing broth as described above.
783 The supernatants were collected after 16 h incubation by centrifugation of the culture at 2,057 g for 10
784 min, followed by filter-sterilization (0.45 μm size). The filter-sterilized supernatant was then
785 ultracentrifuged at 150,000 g for 3 h at 4 ^{o}C to pellet the OMVs. The OMVs were resuspended in
786 phosphate saline buffer (PBS, 9 mM $NaPO_4$, 27 mM NaCl, pH 7.4).
787

Electron microscopy: Electron microscopy images were obtained from the Electron Microscopy unit in the Molecular and Cellular Imaging Facility at the University of Guelph. The OMV samples were negatively stained with 2% uranyl acetate (Chanyi and Koval, 2014; Koval and Hynes, 1991) and visualized using an FEI Tecnai G2 F20 field emission electron microscope operating at 120 kV. Images were obtained using a bottom mount Gatan 4k CCD camera using Tecnai Imaging and Analysis software.

Cellular fractionation: *H. pylori* cells were grown in cyclodextrin-supplemented Brucella broth for 16 h. The cell pellet corresponding to 100 ml of culture was washed 3 times with PBS and resuspended in ice cold 0.5 mM $MgCl_2$ and 30% sucrose to form spheroplasts. Spheroplasts formation was checked by phase contrast microscopy (Leitz Labarlux K) every 20 min over 45-60 min while cells were maintained on ice, and the spheroplasts were pelletted by centrifugation at 4,000 g for 10 min at 4 ^{o}C. The supernatant containing primarily periplasmic protein was reserved on ice. The spheroplasts were lyzed by resuspension in water, addition of acid-washed (and neutralized) glass beads (Sigma, diameter < 106 µm, with a beads /cell suspension ratio of 1/3 (v/v)) with 4 cycles of vortexing for 30 sec and cooling on ice for 30 sec. The cytoplasmic protein fraction was obtained by centrifugation at 12,000 *g* for 30 minutes at 4˚C followed by ultracentrifugation (Beckman) at 100,000 *g* for 1 h. The membranes recovered in the ultracentrifugation pellet were further separated in the inner and outer membrane fractions by differential solubilisation with lauryl sarcosyl (Filip *et al.*, 1973; Hopf *et al.*, 2011). Briefly summarized, the pellet was re-suspended in 50 mM Tris-HCl pH 7.5 containing 1% (w/v) N-lauroyl-sarcosine sodium salt (Sigma) and incubated at room temperature for 1 h. The inner membranes were recovered in the supernatant following ultracentrifugation at 100,000 *g* for 1 h at 4ºC. The outer membrane proteins recovered in the pellet were re-suspended in 50 mM Tris-HCl pH 7.5. All fractions were analyzed by SDS-PAGE (15%), with Coomassie blue staining and anti-HcpE Western blotting.

"Affinity blotting of immobilized substrate" assay to identify folding factors for HcpE: The "affinity blotting of immobilized substrate" assay was adapted from (Wattiau *et al.*, 1994). Purified HcpE-His and control His-TsaA were separated by SDS-PAGE (15%) and transferred to a polyvinylidene difluoride (PVDF) membrane (Roche). Their position on the membrane was determined via Western blotting on a section of the membrane with anti-histidine tag primary antibody (Amersham Biosciences) and goat anti-mouse IgG secondary antibody (Molecular Probes). The remaining section of the membrane was incubated in 10% milk overnight at 4˚C. The membrane was washed 3 times in 50 mM Tris-HCl pH 7.5, containing 150 mM NaCl (TBS) buffer. A soluble cell extract of wild-type *H. pylori* NCTC11637, prepared by mechanical disruption and elimination of insoluble and membrane proteins by ultracentrifugation, was added directly to the membrane and incubated at room temperature for 1 hr. The membrane was then washed 3 times in TBS buffer. Sections of the membrane corresponding to the location of the purified proteins were cut out and subjected to trypsinolysis to recover all peptides stemming from proteins interacting with HcpE or TsaA. The peptides were analyzed by liquid chromatography mass spectrometry (Q-TOF2) at the Protein Identification Facility at the University of Western Ontario as described previously (Hopf *et al.*, 2011).

Refolding assay to assess the ability of DsbK to refold insoluble HcpE: HcpE-His was over-expressed in a 40 ml culture from the pET30a-HcpE-His construct as described above. The cells harvested, re-suspended in 4 ml buffer (50 mM Tris-HCl pH 7.5) and lysed and processed as described above. The insoluble proteins (including HcpE-His) recovered in the centrifugation pellet were re-suspended in 2 ml buffer (50 mM Tris-HCl pH 7.5). Enriched DsbK-Flag, from above, was dialyzed overnight in 50 mM Tris-HCl pH 7.5. The reactions between insoluble HcpE-His and DsbK-Flag were setup in duplicate with 40 µl of insoluble HcpE suspension, 27 µl of DsbK-Flag (undiluted, diluted 1:2, or 1:4) and 3 µl of 1M protease inhibitor cocktail. Reactions with no DsbK-Flag were set-up as negative controls. The reactions were incubated at 37˚C for 1 or 2 h. At each time point, the tubes were

placed on ice for 5 min to stop the reaction and were centrifuged at 10 000 *g* for 10 min at 4˚C. 60 µl of the resulting supernatant, containing the solubilized proteins was carefully removed so as not to disturb the pellet. Solubilized HcpE-His in the supernatants was assessed by Western blotting with anti-HcpE antibodies.

Lysozyme refolding assay: The assay was performed following a previously reported method (Puig and Gilbert, 1994; Puig *et al.*, 1997). Briefly summarized, lysozyme (0.7 mM to 6.7 mM) was denatured and reduced in a total volume of 50 µl comprising 8M urea, 130 mM β-mercaptoethanol, 25 mM Tris-HCl pH 8.6 for 1h 37^{o}C. The sample was diluted 35 fold in 0.1 M acetic acid (final pH 4) to a final concentration of 20-200 µM of lysozyme. For refolding, the sample was further diluted (1.0 to 10 µM lyzozyme) in refolding buffer (5 mM reduced glutathione GSH, 0.5 mM oxidized glutathione GSSG, 100 mM HEPES, pH 7.0, 20 mM NaCl, 2 mM EDTA, 5 mM MgCl2). Refolding was performed in 100 µl reactions and was left to proceed for 1h at 37^{o}C in the presence of 5 µM of purified DsbK-Flag-His, DsbA-Flag-His or DsbG-Flag-His. The reactions were then quenched by addition of an equal volume of 0.1 M acetic acid.

The extent of lyzozyme refolding was then assessed by measuring the lysozyme's lytic activity on the cell wall of *Micrococcus lysodeikticus* (Sigma) as described previously (Puig and Gilbert, 1994). Lysis was monitored spectrophotometrically (as the decrease of turbidity read at 650 nm) over time at 25^{o}C using a 0.5 g/l cell suspension in 100 µl of 60 mM potassium phosphate, 0.1% NaCl, pH 6.2 and a ~2.5 fold dilution of the quenched refolded lysozyme preparation (final lyzozyme concentration 1.0 and 1.5 µM). The assays were performed in triplicates in 96-well plates using an Eon (Bioteck) plate reader. A control reaction was done using the same molarities of native lysozyme that was diluted in the same solutions (0.1 M acetic acid, refolding buffer and lysis reaction buffer) as the refolded one.

Dithiotreitol exposure assays in *E. coli*: DsbK-Flag-His, DsbA-Flag-His, DsbG-Flag-His and GmD-His were over-expressed in *E. coli* BL21(DE3)pLys. Protein expression was induced with 0.1 mM IPTG when the OD_{600nm} reached 0.5 and was allowed to proceed for 3 h at 37°C. Control non-induced cultures were grown in parallel. Serial dilutions of all cultures were then spotted (10 µl) in duplicates on LB agar plates containing 0, 5, 7.5 or 10 mM dithiothreitol (DTT) in the presence or absence of 0.1 mM IPTG. The plates also contained the kanamycin at 30 µg/ml and chloramphenicol at 34 µg/ml to maintain the expression plasmid and the pLys episome. Growth was assessed after overnight incubation at 37°C. Protein expression was assessed by anti-His Western blotting on the pre-induced cultures before plate spotting and on cells recovered from the plates after overnight growth. Similarly, pre-induced or control cultures were inoculated at a 1/4000 dilution (100 µl total) in the wells of a Bioscreen plate in the presence of 0, 7.5 or 10 mM DTT supplemented with 0.1 mM IPTG or not. Growth was monitored automatically over 24 h at 37°C under agitation. Protein expression was assessed by anti-His Western blotting on the pre-induced cultures before inoculation of the Bioscreen plate and from 10 ul aliquotes withdrawn from the bioscreen plate at 6 h and 24 h of incubation.

Dithiotreitol and hydrogen peroxide (H_2O_2) exposure assays in *H. pylori*: *H. pylori* NCTC11637 wild-type and *dsbK* and *hcpE* mutants were revived from freezer stocks as a ~ 1cm diameter spot on a Brucella plate containing background antibiotics and appropriate selection. After 48 h of incubation, the cells were expanded onto a full plate. After 48 h of incubation, the cells were harvested in Brucella broth. For the DTT assay, their OD_{600nm} was adjusted to 0.5, the cells were then serial diluted by 10 fold and spot plated (10 µl) on plates containing 0, 8, 10 or 12 mM dithiotreitol (DTT). For the H_2O_2 assay, the OD_{600nm} was adjusted to 1. Aliquotes of 100 µl were then diluted by an equal volume of broth containing 150, 200 or 250 mM H_2O_2. After 30 min incubation, the bacteria were serial diluted

885 (10-fold intervals) and spotted on blood agar plates. Growth was performed under microaerobic
886 conditions.
887
888
889 **Acknowledgements:** We thank Ryan Chanyi and Dr S. Koval from Western University (Microbiology
890 and Immunology) and the Electron Microscopy unit of the Molecular and Cellular Imaging Facility at
891 the University of Guelph for the EM analysis of OMVs. We thank A. Merkx-Jacques, M. Demendi and
892 L. Meng for cloning His-TsaA, GmD-His and HP0231-His in the pET vector.
893 This work was funded via a CIHR-Gastroenterology operating grant (MOP 105026 2010-2012)
894 administered via the Canadian Association of Gastroenterology (CAG) and financed via CIHR and
895 Astra-Zeneca, a Gap funding grant from the Schulich School of Medicine and Dentistry (2012), a
896 Professional Development Mini-Fellowship (2011) from the University of Western Ontario and an
897 equipment grant (spectrophotometer and plate reader, 2011) from the Academic Development Fund of
898 the University of Western Ontario. Partial support for graduate students S. Kichler, J. Chahal and J.
899 Lester was provided by the School for Graduate and Post-doctoral Studies and the Schulich School of
900 Medicine and Dentistry of Western University. L. Meng and A. Merkx-Jacques were recipients of
901 CAG summer and PhD scholarships, respectively. A. Oberc was the recipient of an NSERC-USRA
902 scholarship.
903
904
905

906 **References:**

907

908

909 Albert, T.J., Dailidiene, D., Dailide, G., Norton, J.E., Kalia, A., Richmond, T.A., Molla, M., Singh, J.,
910 Green, R.D., and Berg, D.E. (2005) Mutation discovery in bacterial genomes: metronidazole
911 resistance in *Helicobacter pylori*. *Nat Methods* **2**: 951-953.
912 Alm, R.A., Ling, L.S., Moir, D.T., King, B.L., Brown, E.D., Doig, P.C., Smith, D.R., Noonan, B.,
913 Guild, B.C., deJonge, B.L., Carmel, G., Tummino, P.J., Caruso, A., Uria-Nickelsen, M., Mills,
914 D.M., Ives, C., Gibson, R., Merberg, D., Mills, S.D., Jiang, Q., Taylor, D.E., Vovis, G.F., and
915 Trust, T.J. (1999) Genomic-sequence comparison of two unrelated isolates of the human gastric
916 pathogen *Helicobacter pylori*. *Nature* **397**: 176-180.
917 Andersen, C.L., Matthey-Dupraz, A., Missiakas, D., and Raina, S. (1997) A new *Escherichia coli* gene,
918 *dsbG*, encodes a periplasmic protein involved in disulphide bond formation, required for
919 recycling DsbA/DsbB and DsbC redox proteins. *Mol Microbiol* **26**: 121-132.
920 Austin, J.W., Doig, P., Stewart, M., and Trust, T.J. (1991) Macromolecular structure and aggregation
921 states of *Helicobacter pylori* urease. *J Bacteriol* **173**: 5663-5667.
922 Backert, S., and Clyne, M. (2011) Pathogenesis of *Helicobacter pylori* infection. *Helicobacter* **16**
923 **Suppl 1**: 19-25.
924 Bardwell, J.C., McGovern, K., and Beckwith, J. (1991) Identification of a protein required for disulfide
925 bond formation in vivo. *Cell* **67**: 581-589.
926 Basso, D., Plebani, M., and Kusters, J.G. (2010) Pathogenesis of *Helicobacter pylori* infection.
927 *Helicobacter* **15 Suppl 1**: 14-20.
928 Bennett, J.C., and Hughes, C. (2000) From flagellum assembly to virulence: the extended family of
929 type III export chaperones. *Trends Microbiol* **8**: 202-204.
930 Bennett, J.C., Thomas, J., Fraser, G.M., and Hughes, C. (2001) Substrate complexes and domain
931 organization of the Salmonella flagellar export chaperones FlgN and FliT. *Mol Microbiol* **39**:
932 781-791.
933 Bessette, P.H., Cotto, J.J., Gilbert, H.F., and Georgiou, G. (1999) *In vivo* and *in vitro* function of the
934 *Escherichia coli* periplasmic cysteine oxidoreductase DsbG. *J Biol Chem* **274**: 7784-7792.
935 Bumann, D., Aksu, S., Wendland, M., Janek, K., Zimny-Arndt, U., Sabarth, N., Meyer, T.F., and
936 Jungblut, P.R. (2002) Proteome analysis of secreted proteins of the gastric pathogen
937 *Helicobacter pylori*. *Infect Immun* **70**: 3396-3403.
938 Butty, F.D., Aucoin, M., Morrison, L., Ho, N., Shaw, G.S., and Creuzenet, C. (2009) Elucidating the
939 formation of 6-deoxyheptose: biochemical characterization of the GDP-D-glycero-D-*manno*-
940 heptose C6 dehydratase, DmhA and its associated C4 reductase, DmhB. *Biochemistry* **48**: 7764-
941 7775.
942 Cao, P., McClain, M.S., Forsyth, M.H., and Cover, T.L. (1998) Extracellular release of antigenic
943 proteins by *Helicobacter pylori*. *Infect Immun* **66**: 2984-2986.
944 Chanyi, R.M., and Koval, S.F. (2014) Role of Type IV pili in predation by *Bdellovibrio bacteriovorus*
945 *PLOS ONE* **Accepted.**
946 Cheng, K.S., Lu, M.C., Tang, H.L., and Chou, F.T. (2002) Phosphorylation of *Helicobacter pylori*
947 CagA in patients with gastric ulcer and gastritis. *Adv Ther* **19**: 85-90.
948 Cheung, J., Goodman, K., Munday, R., Heavner, K., Huntington, J., Morse, J., Veldhuyzen van Zanten,
949 S., Fedorak, R.N., Corriveau, A., and Bailey, R.J. (2008) *Helicobacter pylori* infection in
950 Canada's arctic: searching for the solutions. *Can J Gastroenterol* **22**: 912-916.

Christofides, A., Schauer, C., and Zlotkin, S.H. (2005) Iron deficiency and anemia prevalence and associated etiologic risk factors in First Nations and Inuit communities in Northern Ontario and Nunavut. *Can J Public Health* **96**: 304-307.

Clyne, M., Labigne, A., and Drumm, B. (1995) *Helicobacter pylori* requires an acidic environment to survive in the presence of urea. *Infect Immun* **63**: 1669-1673.

Deml, L., Aigner, M., Decker, J., Eckhardt, A., Schutz, C., Mittl, P.R., Barabas, S., Denk, S., Knoll, G., Lehn, N., and Schneider-Brachert, W. (2005) Characterization of the *Helicobacter pylori* cysteine-rich protein A as a T-helper cell type 1 polarizing agent. *Infect Immun* **73**: 4732-4742.

Depuydt, M., Leonard, S.E., Vertommen, D., Denoncin, K., Morsomme, P., Wahni, K., Messens, J., Carroll, K.S., and Collet, J.F. (2009) A periplasmic reducing system protects single cysteine residues from oxidation. *Science* **326**: 1109-1111.

Devi, V.S., Sprecher, C.B., Hunziker, P., Mittl, P.R., Bosshard, H.R., and Jelesarov, I. (2006) Disulfide formation and stability of a cysteine-rich repeat protein from *Helicobacter pylori*. *Biochemistry* **45**: 1599-1607.

Devi, V.S., and Mittl, P.R. (2011) Monitoring the disulfide bond formation of a cysteine-rich repeat protein from *Helicobacter pylori* in the periplasm of *Escherichia coli*. *Curr Microbiol* **62**: 903-907.

Donahue, J.P., Israel, D.A., Peek, R.M., Blaser, M.J., and Miller, G.G. (2000) Overcoming the restriction barrier to plasmid transformation of *Helicobacter pylori*. *Mol Microbiol* **37**: 1066-1074.

Dumrese, C., Slomianka, L., Ziegler, U., Choi, S.S., Kalia, A., Fulurija, A., Lu, W., Berg, D.E., Benghezal, M., Marshall, B., and Mittl, P.R. (2009) The secreted Helicobacter cysteine-rich protein A causes adherence of human monocytes and differentiation into a macrophage-like phenotype. *FEBS Lett* **583**: 1637-1643.

Dutton, R.J., Boyd, D., Berkmen, M., and Beckwith, J. (2008) Bacterial species exhibit diversity in their mechanisms and capacity for protein disulfide bond formation. *Proc Natl Acad Sci U S A* **105**: 11933-11938.

Eyles, S.J., Radford, S.E., Robinson, C.V., and Dobson, C.M. (1994) Kinetic consequences of the removal of a disulfide bridge on the folding of hen lysozyme. *Biochemistry* **33**: 13038-13048.

Ferlay, J., Shin, H.R., Bray, F., Forman, D., Mathers, C., and Parkin, D.M. (2010) Estimates of worldwide burden of cancer in 2008: GLOBOCAN 2008. *Int J Cancer* **127**: 2893-2917.

Filip, C., Fletcher, G., Wulff, J.L., and Earhart, C.F. (1973) Solubilization of the cytoplasmic membrane of *Escherichia coli* by the ionic detergent sodium-lauryl sarcosinate. *J Bacteriol* **115**: 717-722.

Forman, D., and Burley, V.J. (2006) Gastric cancer: global pattern of the disease and an overview of environmental risk factors. *Best Pract Res Clin Gastroenterol* **20**: 633-649.

Fraser, G.M., Bennett, J.C., and Hughes, C. (1999) Substrate-specific binding of hook-associated proteins by FlgN and FliT, putative chaperones for flagellum assembly. *Mol Microbiol* **32**: 569-580.

Ge, Z., and Taylor, D.E. (1997) *H. pylori* DNA Transformation by Natural Competence and Electroporation. *Methods Mol Med* **8**: 145-152.

Godlewska, R., Dzwonek, A., Mikula, M., Ostrowski, J., Pawlowski, M., Bujnicki, J.M., and Jagusztyn-Krynicka, E.K. (2006) *Helicobacter pylori* protein oxidation influences the colonization process. *Int J Med Microbiol* **296**: 321-324.

Goodman, K.J., Jacobson, K., and Veldhuyzen van Zanten, S. (2008) *Helicobacter pylori* infection in Canadian and related Arctic Aboriginal populations. *Can J Gastroenterol* **22**: 289-295.

Grant, B., and Greenwald, I. (1996) The *Caenorhabditis elegans sel-1* gene, a negative regulator of lin-12 and glp-1, encodes a predicted extracellular protein. *Genetics* **143**: 237-247.

Guilhot, C., Jander, G., Martin, N., and Beckwith, J. (1995) Evidence that the pathway of disulfide bond formation in *Escherichia coli* involves interactions between the cysteines of DsbB and DsbA. *Proc Natl Acad Sci U S A.* **21**: 9895-9899.

Haas, G., Karaali, G., Ebermayer, K., Metzger, W.G., Lamer, S., Zimny-Arndt, U., Diescher, S., Goebel, U.B., Vogt, K., Roznowski, A.B., Wiedenmann, B.J., Meyer, T.F., Aebischer, T., and Jungblut, P.R. (2002) Immunoproteomics of *Helicobacter pylori* infection and relation to gastric disease. *Proteomics* **2**: 313-324.

Harata, K. (1994) X-ray structure of a monoclinic form of hen egg-white lysozyme crystallized at 313 K. Comparison of two independent molecules. *Acta Crystallogr D Biol Crystallogr* **50**: 250-257.

Hawtin, P.R., Stacey, A.R., and Newell, D.G. (1990) Investigation of the structure and localization of the urease of *Helicobacter pylori* using monoclonal antibodies. *J Gen Microbiol* **136**: 1995-2000.

Helicobacter and Cancer Collaborative Group (2001) Gastric cancer and *Helicobacter pylori*: a combined analysis of 12 case control studies nested within prospective cohorts. *Gut* **49**: 347-353.

Heras, B., Shouldice, S.R., Totsika, M., Scanlon, M.J., Schembri, M.A., and Martin, J.L. (2009) DSB proteins and bacterial pathogenicity. *Nat Rev Microbiol* **7**: 215-225.

Heuermann, D., and Haas, R. (1998) A stable shuttle vector system for efficient genetic complementation of *Helicobacter pylori* strains by transformation and conjugation. *Mol Gen Genet* **257**: 519-528.

Hiniker, A., and Bardwell, J.C. (2004) *In vivo* substrate specificity of periplasmic disulfide oxidoreductases. *J Biol Chem* **279**: 12967-12973.

Hopf, P.S., Ford, R.S., Zebian, N., Merkx-Jacques, A., Vijayakumar, S., Ratnayake, D., Hayworth, J., and Creuzenet, C. (2011) Protein Glycosylation in *Helicobacter pylori*: Beyond the Flagellins? *PLoS One* **6**: e25722.

Jameson-Lee, M., Garduno, R.A., and Hoffman, P.S. (2011) DsbA2 (27 kDa Com1-like protein) of *Legionella pneumophila* catalyses extracytoplasmic disulphide-bond formation in proteins including the Dot/Icm type IV secretion system. *Mol Microbiol* **80**: 835-852.

Josenhans, C., Vossebein, L., Friedrich, S., and Suerbaum, S. (2002) The *neuA/flmD* gene cluster of *Helicobacter pylori* is involved in flagellar biosynthesis and flagellin glycosylation. *FEMS Microbiol Lett* **210**: 165-172.

Kaakoush, N.O., Kovach, Z., and Mendz, G.L. (2007) Potential role of thiol:disulfide oxidoreductases in the pathogenesis of *Helicobacter pylori*. *FEMS Immunol Med Microbiol* **50**: 177-183.

Kamitani, S., Akiyama, Y., and Ito, K. (1992) Identification and characterization of an *Escherichia coli* gene required for the formation of correctly folded alkaline phosphatase, a periplasmic enzyme. *EMBO J* **11**: 57-62.

Kapust, R.B., Tozser, J., Fox, J.D., Anderson, D.E., Cherry, S., Copeland, T.D., and Waugh, D.S. (2001) Tobacco etch virus protease: mechanism of autolysis and rational design of stable mutants with wild-type catalytic proficiency. *Protein Eng* **14**: 993-1000.

Kim, N., Weeks, D.L., Shin, J.M., Scott, D.R., Young, M.K., and Sachs, G. (2002) Proteins released by *Helicobacter pylori* in vitro. *J Bacteriol* **184**: 6155-6162.

Koval, S.F., and Hynes, S.H. (1991) Effect of paracrystalline protein surface layers on predation by *Bdellovibrio bacteriovorus*. *J Bacteriol* **173**: 2244-2249.

Kusters, J.G., van Vliet, A.H., and Kuipers, E.J. (2006) Pathogenesis of *Helicobacter pylori* infection. *Clin Microbiol Rev* **19**: 449-490.

Lee, A., O'Rourke, J., De Ungria, M.C., Robertson, B., Daskalopoulos, G., and Dixon, M.F. (1997) A standardized mouse model of *Helicobacter pylori* infection: introducing the Sydney strain. *Gastroenterology* **112**: 1386-1397.

1048 Luthy, L., Grutter, M.G., and Mittl, P.R. (2002) The crystal structure of *Helicobacter pylori* cysteine-
1049 rich protein B reveals a novel fold for a penicillin-binding protein. *J Biol Chem* **277**: 10187-
1050 10193.
1051 Luthy, L., Grutter, M.G., and Mittl, P.R. (2004) The crystal structure of Helicobacter cysteine-rich
1052 protein C at 2.0 A resolution: similar peptide-binding sites in TPR and SEL1-like repeat
1053 proteins. *J Mol Biol* **340**: 829-841.
1054 Marchini, A., d'Apolito, M., Massari, P., Atzeni, M., Copass, M., and Olivieri, R. (1995) Cyclodextrins
1055 for growth of *Helicobacter pylori* and production of vacuolating cytotoxin. *Arch Microbiol* **164**:
1056 290-293.
1057 Marcus, E.A., and Scott, D.R. (2001) Cell lysis is responsible for the appearance of extracellular urease
1058 in *Helicobacter pylori*. *Helicobacter* **6**: 93-99.
1059 McMahon, B.J., Hennessy, T.W., Bensler, J.M., Bruden, D.L., Parkinson, A.J., Morris, J.M.,
1060 Reasonover, A.L., Hurlburt, D.A., Bruce, M.G., Sacco, F., and Butler, J.C. (2003) The
1061 relationship among previous antimicrobial use, antimicrobial resistance, and treatment
1062 outcomes for *Helicobacter pylori* infections. *Ann Intern Med* **139**: 463-469.
1063 Merkx-Jacques, A., Obhi, R.K., Bethune, G., and Creuzenet, C. (2004) The *Helicobacter pylori flaA1*
1064 and *wbpB* genes control lipopolysaccharide and flagellum synthesis and function. *J.*
1065 *Bacteriology* **186**: 2253-2265.
1066 Missiakas, D., Georgopoulos, C., and Raina, S. (1993) Identification and characterization of the
1067 *Escherichia coli* gene *dsbB*, whose product is involved in the formation of disulfide bonds *in*
1068 *vivo*. *Proc Natl Acad Sci U S A* **90**: 7084-7088.
1069 Mittl, P.R., Luthy, L., Hunziker, P., and Grutter, M.G. (2000) The cysteine-rich protein A from
1070 *Helicobacter pylori* is a beta-lactamase. *J Biol Chem* **275**: 17693-17699.
1071 Mittl, P.R., and Schneider-Brachert, W. (2007) Sel1-like repeat proteins in signal transduction. *Cell*
1072 *Signal* **19**: 20-31.
1073 Mullaney, E., Brown, P.A., Smith, S.M., Botting, C.H., Yamaoka, Y.Y., Terres, A.M., Kelleher, D.P.,
1074 and Windle, H.J. (2009) Proteomic and functional characterization of the outer membrane
1075 vesicles from the gastric pathogen *Helicobacter pylori*. *Proteomics Clin Appl* **3**: 785-796.
1076 Natale, P., Bruser, T., and Driessen, A.J. (2008) Sec- and Tat-mediated protein secretion across the
1077 bacterial cytoplasmic membrane--distinct translocases and mechanisms. *Biochim Biophys Acta*
1078 **1778**: 1735-1756.
1079 Naumann, M., and Crabtree, J.E. (2004) *Helicobacter pylori*-induced epithelial cell signalling in gastric
1080 carcinogenesis. *Trends Microbiol* **12**: 29-36.
1081 Newton, D.T., and Mangroo, D. (1999) Mapping the active site of the *Haemophilus influenzae*
1082 methionyl-tRNA formyltransferase: residues important for catalysis and tRNA binding.
1083 *Biochem J* **339 (Pt 1)**: 63-69.
1084 O'Connor, P.M., Lapointe, T.K., Jackson, S., Beck, P.L., Jones, N.L., and Buret, A.G. (2011)
1085 *Helicobacter pylori* activates calpain via toll-like receptor 2 to disrupt adherens junctions in
1086 human gastric epithelial cells. *Infect Immun* **79**: 3887-3894.
1087 Olofsson, A., Vallstrom, A., Petzold, K., Tegtmeyer, N., Schleucher, J., Carlsson, S., Haas, R., Backert,
1088 S., Wai, S.N., Grobner, G., and Arnqvist, A. (2010) Biochemical and functional
1089 characterization of *Helicobacter pylori* vesicles. *Mol Microbiol* **77**: 1539-1555.
1090 Parker, H., and Keenan, J.I. (2012) Composition and function of *Helicobacter pylori* outer membrane
1091 vesicles. *Microbes Infect* **14**: 9-16.
1092 Parkin, D.M., Bray, F., Ferlay, J., and Pisani, P. (2005) Global cancer statistics, 2002. *CA Cancer J*
1093 *Clin* **55**: 74-108.
1094 Poole, L.B. (2005) Bacterial defenses against oxidants: mechanistic features of cysteine-based
1095 peroxidases and their flavoprotein reductases. *Arch Biochem Biophys* **433**: 240-254.

Prinz, W.A., Aslund, F., Holmgren, A., and Beckwith, J. (1997) The role of the thioredoxin and glutaredoxin pathways in reducing protein disulfide bonds in the *Escherichia coli* cytoplasm. *J Biol Chem* **272**: 15661-15667.

Puig, A., and Gilbert, H.F. (1994) Protein disulfide isomerase exhibits chaperone and anti-chaperone activity in the oxidative refolding of lysozyme. *J Biol Chem* **269**: 7764-7771.

Puig, A., Primm, T.P., Surendran, R., Lee, J.C., Ballard, K.D., Orkiszewski, R.S., Makarov, V., and Gilbert, H.F. (1997) A 21-kDa C-terminal fragment of protein-disulfide isomerase has isomerase, chaperone, and anti-chaperone activities. *J Biol Chem* **272**: 32988-32994.

Puls, J., Fischer, W., and Haas, R. (2002) Activation of *Helicobacter pylori* CagA by tyrosine phosphorylation is essential for dephosphorylation of host cell proteins in gastric epithelial cells. *Mol Microbiol* **43**: 961-969.

Raczko, A.M., Bujnicki, J.M., Pawlowski, M., Godlewska, R., Lewandowska, M., and Jagusztyn-Krynicka, E.K. (2005) Characterization of new DsbB-like thiol-oxidoreductases of *Campylobacter jejuni* and *Helicobacter pylori* and classification of the DsbB family based on phylogenomic, structural and functional criteria. *Microbiology* **151**: 219-231.

Rain, J.C., Selig, L., De Reuse, H., Battaglia, V., Reverdy, C., Simon, S., Lenzen, G., Petel, F., Wojcik, J., Schachter, V., Chemama, Y., Labigne, A., and Legrain, P. (2001) The protein-protein interaction map of *Helicobacter pylori*. *Nature* **409**: 211-215.

Raju, D., Hussey, S., Ang, M., Terebiznik, M.R., Sibony, M., Galindo-Mata, E., Gupta, V., Blanke, S.R., Delgado, A., Romero-Gallo, J., Ramjeet, M.S., Mascarenhas, H., Peek, R.M., Correa, P., Streutker, C., Hold, G., Kunstmann, E., Yoshimori, T., Silverberg, M.S., Girardin, S.E., Philpott, D.J., El Omar, E., and Jones, N.L. (2012) Vacuolating cytotoxin and variants in Atg16L1 that disrupt autophagy promote *Helicobacter pylori* infection in humans. *Gastroenterology* **142**: 1160-1171.

Raymond, J., Lamarque, D., Kalach, N., Chaussade, S., and Burucoa, C. (2010) High level of antimicrobial resistance in French *Helicobacter pylori* isolates. *Helicobacter* **15**: 21-27.

Rogers, A.B., Taylor, N.S., Whary, M.T., Stefanich, E.D., Wang, T.C., and Fox, J.G. (2005) *Helicobacter pylori* but not high salt induces gastric intraepithelial neoplasia in B6129 mice. *Cancer Res* **65**: 10709-10715.

Roschitzki, B., Schauer, S., and Mittl, P.R. (2011) Recognition of host proteins by Helicobacter cysteine-rich protein C. *Curr Microbiol* **63**: 239-249.

Roszczenko, P., Radomska, K.A., Wywial, E., Collet, J.F., and Jagusztyn-Krynicka, E.K. (2012) A novel insight into the oxidoreductase activity of *Helicobacter pylori* HP0231 protein. *PLoS One* **7**: e46563.

Sabarth, N., Hurwitz, R., Meyer, T.F., and Bumann, D. (2002) Multiparameter selection of *Helicobacter pylori* antigens identifies two novel antigens with high protective efficacy. *Infect Immun* **70**: 6499-6503.

Sambrook, J., Fritsch, E.F., and Maniatis, T. (1989) Molecular cloning: a laboratory manual. *Cold Spring Harbor Laboratory, Cold Spring Harbor, N.Y.*

Shao, F., Bader, M.W., Jakob, U., and Bardwell, J.C. (2000) DsbG, a protein disulfide isomerase with chaperone activity. *J Biol Chem* **275**: 13349-13352.

Sinha, S.K., Martin, B., Gold, B.D., Song, Q., Sargent, M., and Bernstein, C.N. (2004) The incidence of *Helicobacter pylori* acquisition in children of a Canadian First Nations community and the potential for parent-to-child transmission. *Helicobacter* **9**: 59-68.

Tomb, J.F., White, O., Kerlavage, A.R., Clayton, R.A., Sutton, G.G., Fleischmann, R.D., Ketchum, K.A., Klenk, H.P., Gill, S., Dougherty, B.A., Nelson, K., Quackenbush, J., Zhou, L., Kirkness, E.F., Peterson, S., Loftus, B., Richardson, D., Dodson, R., Khalak, H.G., Glodek, A., McKenney, K., Fitzegerald, L.M., Lee, N., Adams, M.D., Venter, J.C., and et al. (1997) The complete genome sequence of the gastric pathogen *Helicobacter pylori*. *Nature* **388**: 539-547.

Uemura, N., Okamoto, S., Yamamoto, S., Matsumura, N., Yamaguchi, S., Yamakido, M., Taniyama, K., Sasaki, N., and Schlemper, R.J. (2001) *Helicobacter pylori* infection and the development of gastric cancer. *N Engl J Med* **345**: 784-789.

Urgesi, R., Pelecca, G., Cianci, R., Masini, A., Zampaletta, C., Riccioni, M., and Faggiani, R. (2011) *Helicobacter pylori* infection: is sequential therapy superior to standard triple therapy? A single-centre Italian study in treatment-naive and non-treatment-naive patients. *Can J Gastroenterol.* **25**: 315-318.

van Straaten, M., Missiakas, D., Raina, S., and Darby, N.J. (1998) The functional properties of DsbG, a thiol-disulfide oxidoreductase from the periplasm of *Escherichia coli*. *FEBS Lett* **428**: 255-258.

Vanet, A., and Labigne, A. (1998) Evidence for specific secretion rather than autolysis in the release of some *Helicobacter pylori* proteins. *Infect Immun* **66**: 1023-1027.

Watanabe, T., Tada, M., Nagai, H., Sasaki, S., and Nakao, M. (1998) *Helicobacter pylori* infection induces gastric cancer in mongolian gerbils. *Gastroenterology* **115**: 642-648.

Wattiau, P., Bernier, B., Deslee, P., Michiels, T., and Cornelis, G.R. (1994) Individual chaperones required for Yop secretion by Yersinia. *Proc Natl Acad Sci U S A* **91**: 10493-10497.

Yamaoka, Y. (2010) Mechanisms of disease: *Helicobacter pylori* virulence factors. *Nat Rev Gastroenterol Hepatol* **7**: 629-641.

Yoon, J.Y., Kim, J., Lee, S.J., Kim, H.S., Im, H.N., Yoon, H.J., Kim, K.H., Kim, S.J., Han, B.W., and Suh, S.W. (2011) Structural and functional characterization of *Helicobacter pylori* DsbG. *FEBS Lett* **585**: 3862-3867.

Table I: List of Hcp family members and their main characteristics.

Name (ORF)	# AA	MW	# Cys	% Cys	Structure modeled onto:	# SLRs	Disulfide bonds
Hcp A (HP0211)	250	27.4	14	5.6	HcpC	6	Yes
Hcp B (HP0336)	138	15.3	8	5.8	HcpB structure known (Luthy *et al.*, 2002)	4	Yes
Hcp C (HP1098)	290	31.6	16	5.5	HcpC structure known (Luthy *et al.*, 2004)	7	Yes
Hcp D (HP0160)	306	34.1	15	4.9	HcpC	7	Yes
Hcp E (HP0235)	355	39.4	19	5.4	HcpC	9	Yes
Hcp F (HP0628)	225	24.6	12	5.3	HcpC	5	Yes
Hcp G (HP1117)	256	29.0	5	2.0	HcpC	5	No

ORF: open reading frame; # AA: number of amino acids; MW: Molecular weight; # Cys: number of cysteine residues; % Cys: percent of cysteine residues; # SLRS: number of SLR repeats.

Modeling was done using Swiss-Prot.

Table II: Protein hits obtained by mass spectrometry from bands corresponding to full length HcpE, truncated HcpE or control TsaA protein using the "affinity of immobilized substrate" technique. After pure HcpE-His or TsaA-His were run on a gel, they were transferred onto a PVDF membrane. A section of the membrane was used for Western blotting to locate the proteins. The rest of the membrane was incubated with a wild-type *H. pylori* soluble protein extract. After extensive washing, bands corresponding to the location of TsaA or HcpE (full length or truncated) were excised and subjected to trypsinolysis to extract peptides of proteins interacting with TsaA or HcpE and the peptides were analysed by MS. The molecular weight of the band extracted for MS analysis is indicated for each sample. For each hit, the number of unique peptides matched to the hit sequence is indicated (top number) as well as the percentage of sequence coverage (bottom number in brackets). PPI stands for peptidyl-prolyl cis/trans isomerase.

Protein hit	MW of hit (kDa)	in TsaA band (~27 kDa)	in truncated HcpE band (~ 30 kDa)	in full length HcpE band (~41 kDa)
PPI	34	None	2 (6)	None
DnaK	67	8 (21)	None	2 (4)
GroEL	58	19 (47)	6 (16)	7 (19)
GroES	13.0	None	3 (24)	None
Thioredoxin	11.8	4 (56)	2 (23)	1 (9)
TsaA (AhpC)	22.3	15 (88)	9 (49)	9 (44)
HP0235 (HcpE)	39.4	None	None	3 (9)
HP0231 (DsbK)	29.5	None	1 (4)	1 (4)

1192 **Table III: List of nucleotide sequences for primers.**

1193

Primer name	Sequence (5' to 3')
HP0231P1	GGAAGAC**CATATG**ATATTAAGAGCGAGTGTG
HP0231P2	CG**GGATCC**T**GCTAGC**TCACTTGTCGTCGTCGTCCTTGTAGTC**AGAGC C**TGCCTTATAATGGTATAAGAAAG
HP0231P3	GCG**GGATCC**GGACTGAAAATACAAATTCTCCTTGTCGTCGTCGTCCT TGTA
HP0231P4	CGC**GGATCC**CACCACCACCACCACCACTG
HP0231P5	CCG**G/AATTC**ATG ATATTAAGAGCGAGTGTGTTG
HP0231P6	CC**AT/CGAT**GAGCTCACTAAACTTAGGGATC
HP0231P7	CC**GGTACC**GGTGGCGTTAAGAGCTTGAAC
231Comp1	GTGA**CTGCAG**GGGATAAGGGAGCGCGA
231Comp2	ATG**GAATTC**CGTTGGGCGTTTTGCTGG
231Comp3	CGT**GGATCC**TATAAGGTTGCTCTCATGAAAAAACC
231Comp4	CTG**TCTAGA**TCAGTGGTGGTGGTGGTGGTGTGCCTTATAATGGTATA AGAAAGG
HP0230P2	TCGCCTTGCAAGTTTAAAACCC
HP0232P3	CTGAC**CCATGG**ATAGGGATGAGCGCGCGTTTAGG
HP0235P1	CTC**GAATTT**AGAGCATAAAGAAGAGCGTAAG
HP0235P2	CTC**GAATTC**TCAATACCCCCTAAGTTTAGTG
HP0235P4	CC**ATCGAT**GAAGATTTTGAAGTGGCG
HP0235P5	GA**AGATCT**ATTCTAGTGCCTTGCCC
HP0235P8	GGAAGAC**CATATG**GGTGTCAAATTTTTAAAAATATTAG
HP0235P9	ATAGTTTCGC**GGCCGC**ATACCCCCTAAGTTTAGTGAGGT
HP0235P10	CAAGGGGATAAAACTAAAGCG
DsbAEcP1	GGAAGAC**CATATG**AAAAAGATTTGGCTGGCGC
DsbAEcP2	GCG**GGATCC**GGACTGAAAATACAAATTCTCCTTGTCGTCGTCGTCCT TGTAGTCAGAGCCTTTTTTCTCGGACAGATATTTCAC
DsbGEcP1	GGAAGAC**CATATG**TTAAAAAAGATACTTTTACTGGC
DsbGEcP2	GCG**GGATCC**GGACTGAAAATACAAATTCTCCTTGTCGTCGTCGTCCT TGTAGTCAGAGCCTTTATTCCCCATAATGATATTAAGC
CJ1319P9	GGAAGAC**CATATG**GATGGAAAGGGTGA
CJ1319P10	GCCG**CTCGAG**AACATTATAAAGTTCGCTT
HP1563P7	CCTGT**ACATGT**GCATGTTAGTTACAAAACTTGC
HP1563P2	ACTCT**GGATCC**TTAAAGCTTAATGGAATTTTC
Aph3P1	GA**AGATCT**GATAAACCCAGCGAACCA
Aph3P2	CC**ATCGAT**AGACATCTAAATCTAGGTAC
Aph3P4	CC**GGTACC**GATAAACCCAGCGAACCAT
CatHelP1	GC**TCTAGA**CTCAAAACGATGAAATAGGGC
CatHelP2	GA**GGATCC**CCGGGTACCG
CtermHis	CG**GGATCC**TCAGTGGTGGTGGTGGTGG
T7ProX	TAATACGACTCA**CTATAG**GGG
HPFlagBP5	CAG**GGATCC**ATGGAACGCCTTTAATAAAATG
HPFlagBP7	CACGAATTCTCAGTGGTGGTGGTGGTGGTGACTTCCGGA**CATATG**TT GTAAAAGCCTTAAGACATTTTG

HP0954P1	CGGAATTCATGAGTTGCGTTATCCCAGC

* Restriction sites relevant to procedures used in this work are **bolded** and underlined

Figure legends:

Figure 1: HcpE is produced by *H. pylori* strains NCTC11637 and SS1 and is secreted into the culture supernatant.

Panels A and C: Analysis of the production and secretion of HcpE in *H. pylori* strains NCTC11637 (panel A) and SS1 (panel C) wild-type in comparison with their isogenic *hcpE::kan* knockout mutant. A Ponceau S red stain (PR) of the total proteins present in each fraction is provided as a loading control. HcpE was detected by Western blotting (WB) using a polyclonal serum raised in rabbits against purified HcpE. HcpE was detected at the expected ~ 40 kDa in wild-type pellets and supernatants (Sup) but was absent from the knockout mutants in both strains.
Panels B and D: Urease activity assay on the total culture (Tot, strain NCTC11637 only), the cell pellet and the culture supernatant (Sup), used as an indication of absence of cell lysis. Urease activity was determined using the phenol red assay (Clyne *et al.*, 1995). Panel B is for strain NCTC11637, data acquisition of 1 point per min. Panel D is for strain SS1 with 1 point per 2.5 min. Hardly any urease activity was observed with the supernatants.

Figure 2: A portion of secreted HcpE is found in outer membrane vesicles. Panel A: SDS-PAGE analysis of the pellets obtained by ultracentrifugation of filter-sterilized culture supernatants of wild-type, *hcpE*::kan and *dsbK*::kan mutants. Detectiong was done by Coomassie blue staining and by Western blotting with anti-HcpE antibodies. **Panel B:** The same samples as in panel A were treated with proteinase K (+ PK) or not (- PK) before analysis by SDS-PAGE and silver staining. Together, panels A and B show that HcpE is abundant in the wild-type samples, absent from the *hcpE* mutant samples as expected, and its amount is drastically reduced in the *dsbK* mutant despite similar global protein and LPS patterns. **Panel C:** SDS-PAGE analysis of the inner and outer membrane fractions of wild-type, *hcpE*::kan and *dsbK*::kan mutants. Total membranes were first obtained by

ultracentrifugation of mechanically-disrupted whole cells, and the inner and outer membranes were separated by differential solubilisation in lauryl sarcosyl followed by ultracentrifugation. Coomassie and silver staining of these membrane fractions indicate that the protein and LPS patterns observed in panel B are distinct from inner membranes but are similar to those observed in outer membranes. Therefore, these samples likely represent outer membrane vesicles. **Panel D:** The samples from panels A and B were analyzed by electron microscopy after uranyl acetate staining. Spherical membrane-bound structures of 75 to 150 nm in diameter that are characteristic of outer membrane vesicles were observed in all strains.

Figure 3: Schematic representation of the array of Sel-Like Repeats (SLRs) and cysteines present in HcpE, and 3D structure of a typical SLR. Panel A: mature HcpE comprises nine SLRs, each containing two alpha helices (cylinders a and b). Each helix contains one cysteine (C). The signal peptide also contains one cysteine that is eliminated from mature HcpE upon cleavage of the signal peptide. **Panel B**: modeled 3D structure of an SLR. The two alpha helices of the SLR motif are maintained in a V-shape structure via a disulfide bond.

Figure 4: Structures of HcpC and HcpE. Panel A: known crystal structure of HcpC (Luthy *et al.*, 2004). **Panel B:** Direct modeling of full-length HcpE onto the HcpC structure using SwissProt. This modeling was not successful due to the much larger size of HcpE compared with HcpC. Helices that are not modeled within the regular array of SLR motifs are indicated in colors different from the rest of the HcpE protein. **Panel C**: modeling of HcpE as two overlapping moieties (amino acids (AA) 1-230 and 143-355). The overlapping alpha helices are represented in the same color on each protein moiety. **Panel D**: Final reconstituted HcpE structure, once the overlapping alpha helices are aligned using PyMol. The reconstituted HcpE is a solenoid protein and cohesion of its structure in this model relies heavily on formation of disulfide bonds between cysteines from each of the nine SLR motifs.

Figure 5: Structure-based sequence alignments for HcpE and HcpC. The alignments were generated from the modeled HcpE structure shown in Figure 4 and from crystallography data for HcpC (Luthy *et al.*, 2004). # refers to the SLR position within the Hcp sequence. AA: amino acid position in the sequence. ! indicates amino acids conserved in all SLRs for each protein. + indicates conservation of similar types of amino acids in 90-99% of SLRs. * indicates conservation of similar types of amino acids in 70-89% of SLRs. The shaded box highlights the conserved cysteines that are invariably separated by seven residues that form a small loop at the edges of the two intra-SLR alpha helices. The same features apply to HcpE (ORF HP0235) and HcpC. In addition, in HcpC, there is conservation in sequence and length in the linker that separates SRL motifs from one another.

Figure 6: DsbK is important for the production and secretion of HcpE in *H. pylori*. Wild-type and *dsbK* knockout mutant bacteria were subjected to spheroplasting conditions to extract periplasmic proteins. The process of spheroplasting was monitored by dark field microscopy (oil immersion) as loss of typical bacterial "hockey stick" shape of *H. pylori* NCTC11637. The cells were separated from the released soluble proteins by centrifugation. The cells were lyzed by mechanical disruption, debris were pelleted away and the supernatant was ultracentrifuged to obtain the cytoplasmic proteins devoid of membrane components. Separately, the culture supernatants were filter sterilized and ultracentrifuged to pellet the OMVs. **Panel A:** The samples were analyzed by SDS-PAGE followed by Ponceau S red staining (PR) and Western blotting (WB) for the presence of HcpE using anti-HcpE antibodies. The bracket highlights the area of the membrane that was subjected to WB. Densitometry was performed using the Image J software. **Panel B:** Urease activity of the various fractions was monitored to assess cellular lysis (representative example of 3 independent experiments). Abbreviations: Tot: total cells. Sup: culture supernatant. Cytop: cytoplasmic proteins. Perip: periplasmic proteins. Inactivation of *dsbK* clearly leads to reduction in production of HcpE and most of the produced protein appears trapped

within the periplasm, with little release in OMVs. A small amount of urease activity was recovered in the periplasmic fraction, indicating slight contamination by cytoplasmic proteins during the spheroplasting process, which was also apparent from the protein profile. However, the fact that HcpE was only found in the periplasmic fraction of the mutant and not in the cytoplasm indicates that periplasmic enrichment had been achieved and that the protein transits to the periplasm as expected. The low level of HcpE found in the OMVs of the mutant despite efficient secretion of urease to the OMVs suggests that the failure of HcpE to fold in the *dsbK* mutant results in limited export outside the bacterium.

Figure 7: DsbK is necessary to obtain soluble HcpE upon expression in *E. coli.* DsbK and HcpE were co-expressed from the same vector as two independent proteins. Control experiments were performed with HcpE only. After expression at 37°C or room temperature (RT) and mechanical disruption, the soluble proteins and insoluble proteins were separated by centrifugation and analysed by SDS-PAGE with detection by Ponceau S red staining (PR) or anti-HcpE Western blotting (WB). The co-expression of DsbK with HcpE allowed recovery of soluble HcpE when expression was performed at room temperature while no soluble HcpE could be obtained when folding relied on endogenous *E. coli* Dsb proteins only. T: Total cells. S: Soluble proteins. I: Insoluble proteins.

Figure 8: DsbK is able to solubilize denatured and reduced HcpE *in vitro*. Insoluble proteins obtained after over-expression of HcpE in *E. coli* were recovered after mechanical disruption of bacteria and centrifugation removal of soluble proteins. The insoluble proteins comprised two forms of HcpE that migrated at ~ 41 and 39 kDa and that correspond to HcpE with and without its signal peptide (SP). In parallel, DsbK was over-expressed in *E. coli* and enriched by anion exchange chromatography. Control anion exchange fractions eluting at the same salt concentrations as DsbK were obtained using the same *E. coli* background strain that did not express DsbK ("No DsbK" lanes). The insoluble HcpE

protein suspension was incubated with the *E. coli* anion exchange fractions containing over-expressed DsbK or not, the suspension was centrifugated and the supernatant was analyzed for the presence of HcpE by anti-HcpE Western blotting. The Ponceau S red staining panel is provided as a loading control. We observed DsbK-dependent and time-dependent recovery of unprocessed HcpE (i.e. HcpE with signal peptide) in the supernatant, indicating that DsbK facilitated its solubilisation, likely via assisting its folding. PR: Ponceau S red. WB: anti-HcpE Western blot.

Figure 9: DsbK has disulfide bond forming activity on reduced lyzosyme. The ability of lysozyme to lyse micrococci (turbidity decrease) that relies on essential disulfide bonds was monitored as per Puig and Gilbert 1994 (Puig and Gilbert, 1994). **Panels A-C:** common reaction conditions show that addition of *E. coli* DsbG, *E. coli* DsbA or DsbK restored partial activity to reduced and denatured lysozyme (Lys). **Panel D**: optimized assay for DsbK whereby spontaneous refolding of lyzozyme was minimized and addition of DsbK restored activity to reduced and denatured lysozyme (Lys) to levels similar to those obtained with native lysozyme. The process was extremely fast, as opposed to the slow and progressive spontaneous refolding observed in the absence of DsbK. This indicates that the formation of the essential disulfide bonds was facilitated by addition of DsbK.

Figure 10: DsbK has DsbA-like behavior when expressed in *E. coli*. DsbK, *E. coli* DsbA, *E. coli* DsbG, and a control protein (Cj1319) were over-expressed under the same conditions and the cells were serial diluted before spotting on plates (panel A) or inoculation in Bioscreen wells (panel B) containing dithiothreitol (DTT) or not. For the plate assay, three dilutions were spotted in duplicates each as indicated by the triangles and brackets. For the Bioscreen assay, the same dilution was inoculated in 2 wells (with error bars smaller than symbols). **Panel A** indicates that DsbK shows the same deleterious effects as DsbA on bacterial growth, whereby pre-induction of protein expression resulted in less colonies compared with DsbG and the control protein. **Panel B** also shows a DsbA-like

toxic effect of DsbK expression that lengthened the lag phase. This effect was bacteriostatic since growth rates and final culture densities were similar for all strains. For both assays, the effect was exacerbated in the presence of DTT in the growth medium. **Panel C** shows the levels of protein pre-induction attained before inoculating plates or bioscreen wells by Ponceau S red staining (PR) and anti-His Western blotting (WB). DsbK appears highly toxic to the cells since toxicity effects were as high as for DsbA while protein expression levels were 3-4 fold less. Note that the control protein is expressed at very low levels not detectable by anti-His Western blotting.

Figure 11: DsbK is important for survival to redox stress in *H. pylori*. Panel A: Growth of the *dsbK* mutant, *hcpE* mutant and wild-type strain were assessed after growth in broth under microaerobic conditions. The data averaged from 9 independent cultures per strain show that all strains grew to similar cell densities under microaerobic conditions. **Panel B:** The cultures obtained after 24h incubation in panel A were exposed to environmental atmosphere for ~30 min followed by spot plating and further microaerobic incubation. The data are a representative example out of 6 independent experiments, each comprising 3 serial dilutions of each culture spot-plated in triplicates for cfu determinations. The data show a ~0.5-1 log reduction in viability for the *dsbK* mutant, suggesting that it was more sensitive to exposure to oxygen (*: $p<0.001$ for this panel). The effect was not observed for the *hcpE* mutant. **Panel C:** All strains were grown in broth to the same density, and exposed to various concentrations of DTT on plates, or to various concentrations of H_2O_2 before being spotted on regular growth medium to assess viability. All growth was performed under microaerobic conditions. The *dsbK* mutant was impaired for resistance to DTT and H_2O_2 while the *hcpE* mutant was not affected. **Panel D:** Same experiment as in panel C to demonstrate complementation of the phenotype observed for the *dsbK* mutant when the gene was reintroduced in the chromosome (compl.). **Panel E:** quantitation of the colonies recovered in panels C and D. Statistics were performed by ANOVA test

with * for $p<0.05$, ** for $p<0.01$ and *** for $p<0.001$ on this panel. The absence of any * indicates lack of statistical significance.

Lester et al Fig 1

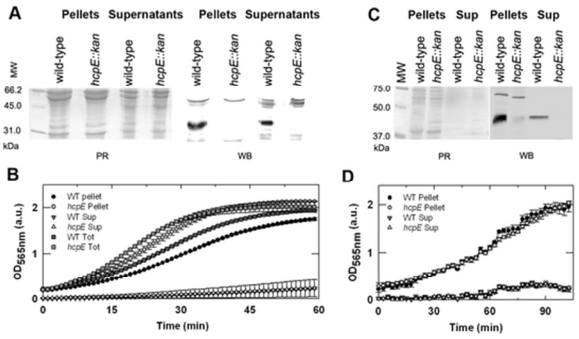

80x53mm (300 x 300 DPI)

Lester et al Fig 2

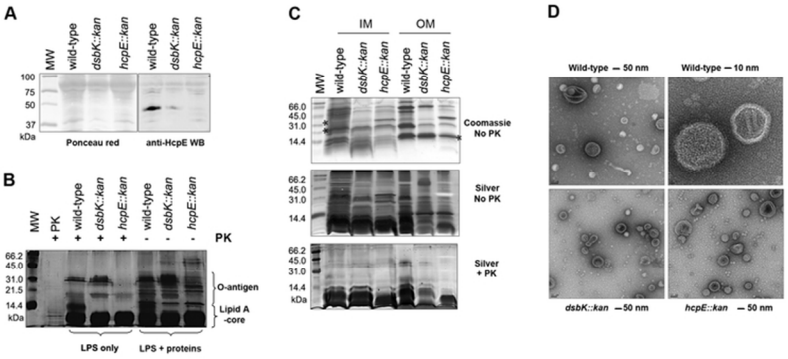

80x53mm (300 x 300 DPI)

Lester et al Fig 3

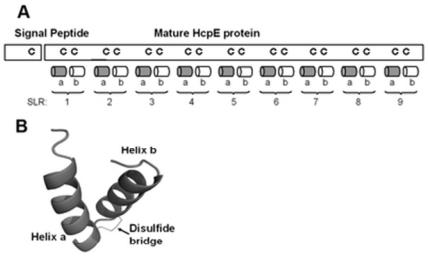

80x53mm (300 x 300 DPI)

Lester et al Fig 4

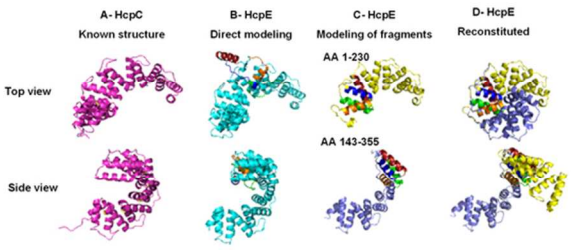

80x53mm (300 x 300 DPI)

Lester et al Figure 5

```
Prot    # AA     -----Helix A---         ---Helix B---
HP0235 1 44     YSKATSYFKKACN-D  GV    SEGCTQLGIIY-E  NGQ-GTRID
HP0235 2 80     YKKALEYYKTACQA-  DD    REGCFGLGGLYDE  -GL-GTTQN
HP0235 3 117    YQEAIDAYAKACVL-  KH    PESCYNLGIIYDR  KIK-GNA--
HP0235 4 152    DQ-AVTYYQKSCNFD  MA    K-GCYVLGVAY-E  KGFLEVKQS
HP0235 5 188    NHKAVIYYLKACRLD  DG    Q-ACRALGSLF-E  NGDAGLDED
HP0235 6 214    FEVAFDYLQKACGL-  NN    SGGCASLGSMYML  -GRY-VKKD
HP0235 7 261    PQKAFNFFKQACDM-  GS    AVSCSRMGFMYSQ  -GDA-VPKD
HP0235 8 297    LRKALDNYERGCDM-  GD    EVGCFALAGMYY-  N-M-KDKEN
HP0235 9 332    AIM--I-YDKGCKL-  GM    KQACENLTK
                  *+  *++**!              !  +*  + *   *     **

HcpC   1 47     -TQAKKYFEKACDL   KE    NSGCFNLGVLYYQ  GQGVEKN
HcpC   2 82     LKKAASFYAKACDL   NY    SNGCHLLGNLYYS  GQGVSQN
HcpC   3 117    TNKALQYYSKACDL   KY    AEGCASLGGIYHD  GKVVTRD
HcpC   4 153    FKKAVEYFTKACDL   ND    GDGCTILGSLYDA  GRGTPKD
HcpC   5 190    LKKALASYDKACDL   KD    SPGCFNAGNMYHH  GEGATKN
HcpC   6 225    FKEALARYSKACEL   EN    GGGCFNLGAMQYN  GEGVTRN
HcpC   7 261    EKQAIENFKKGCKL   GA    KGACDILKQ
                 **!+  + !+!*!   +       +!  ++  +    !*+****
```

215x279mm (200 x 200 DPI)

Lester et al Fig 6

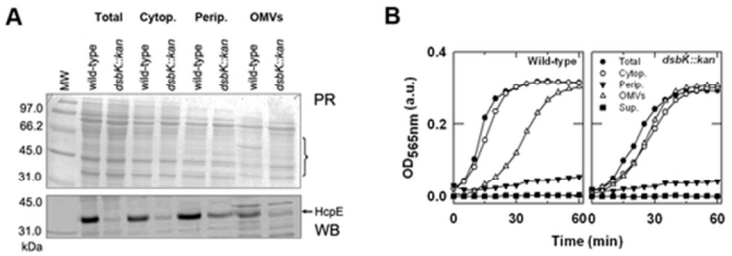

59x39mm (300 x 300 DPI)

Lester et al Fig 7

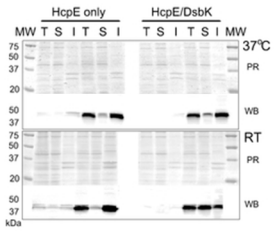

80x53mm (300 x 300 DPI)

Lester et al Fig 8

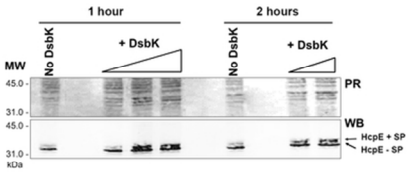

80x53mm (300 x 300 DPI)

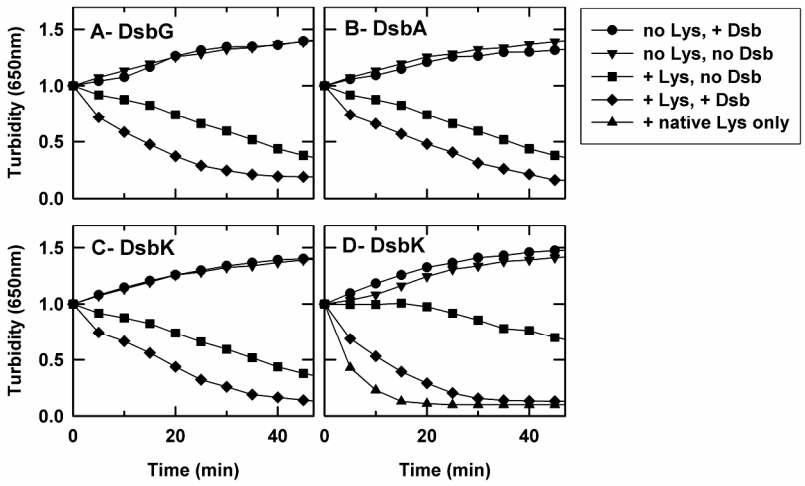

Lester et al Figure 9

279x360mm (300 x 300 DPI)

Lester et al Fig 10

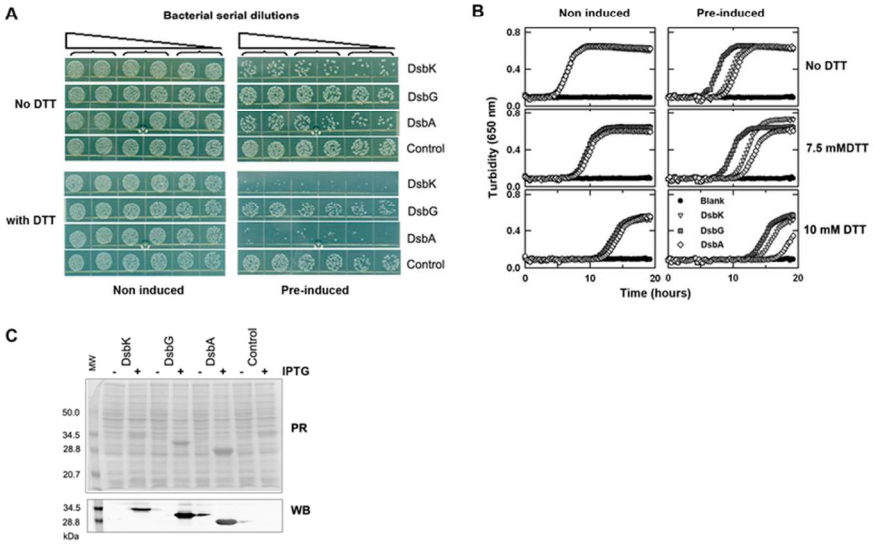

80x53mm (300 x 300 DPI)

Lester et al Fig 11

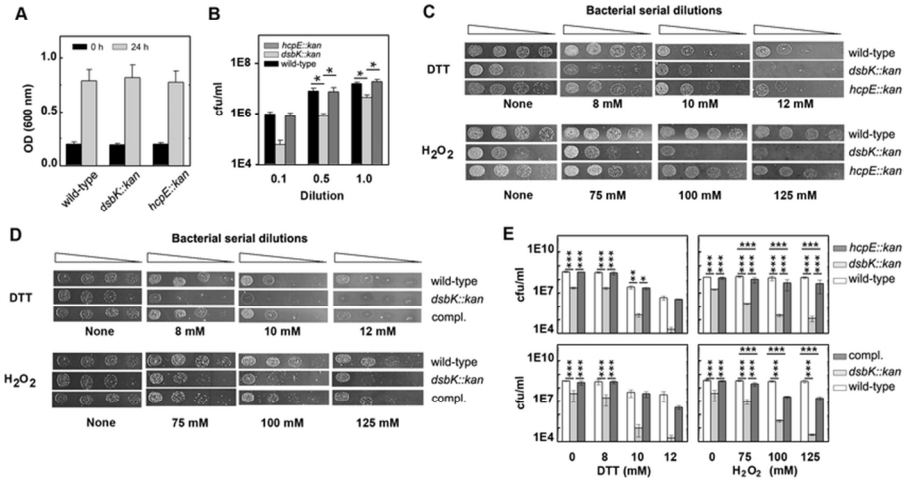

80x53mm (300 x 300 DPI)

Lester et al Fig S1

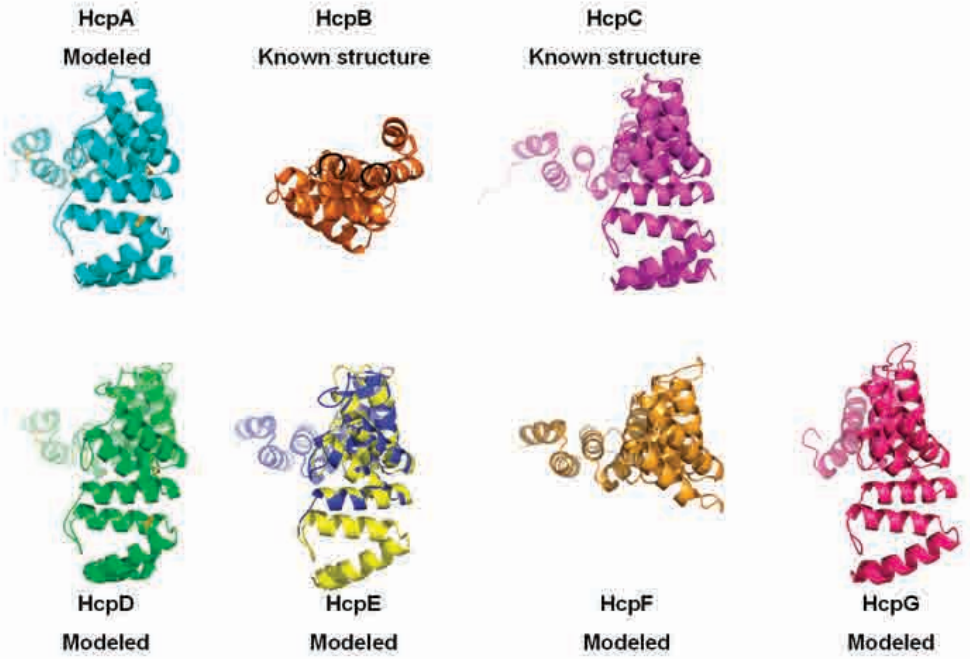

Fig S1: Modeling of the various Hcp proteins reveals modular structure directly related to number of SLR modules present. The structures of HcpB and HcpC were determined experimentally (Luthy et al., 2002, 2004). All other Hcp proteins (except HcpE) comprise less SLR modules than HcpC and could therefore be modeled onto the HcpC structure directly using SwissProt. HcpE was modeled as two overlapping moieties (indicated by 2 colors) as described in Figure 4.

Lester et al Figure S2

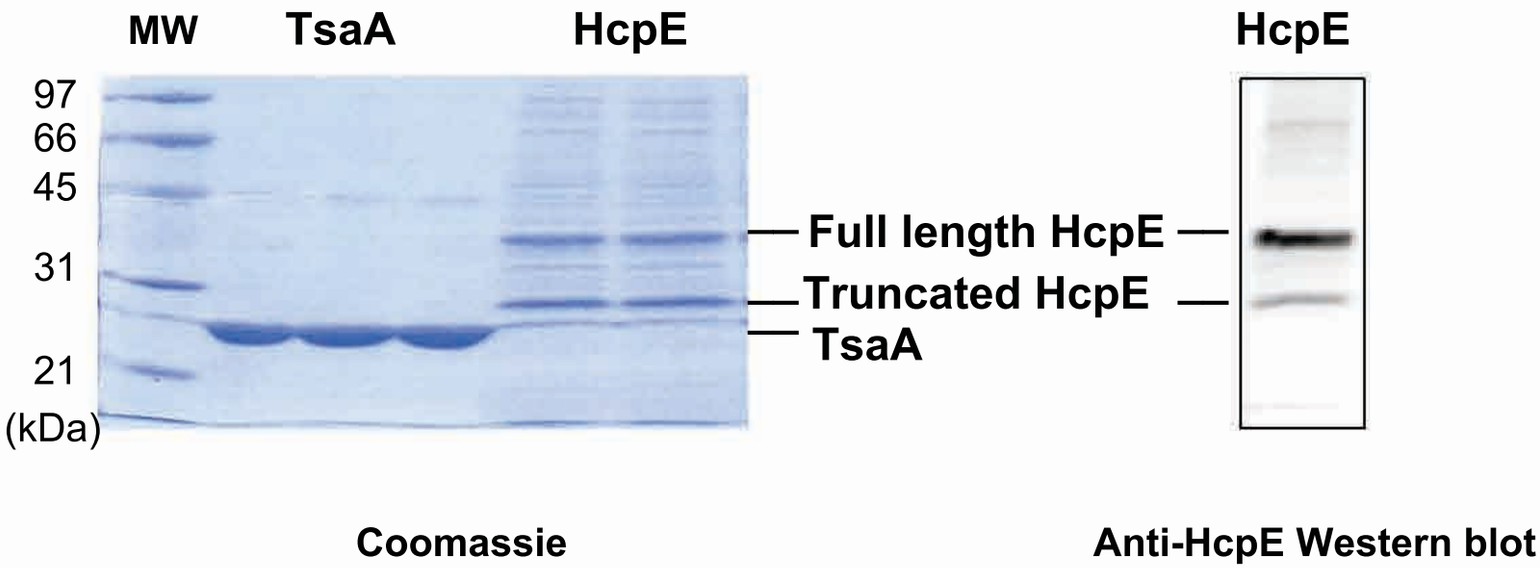

Figure S2: Identification of DsbK as an interacting partner for reduced and denatured HcpE. The technique of "affinity blotting of immobilized substrate" was adapted to identify an interacting partner for reduced and denatured HcpE. The Coomassie-stained gel shows 2 prominent bands in the purified HcpE both reacting with anti-HcpE antibodies and corresponding to full length and truncated HcpE used for this "affinity of immobilized substrate" analysis. It also shows the TsaA protein used as a control. The bands were excised after a replica gel had been trans--ferred onto PVDF and the position of the bands ascertained by Western blotting.

Lester et al Fig S3

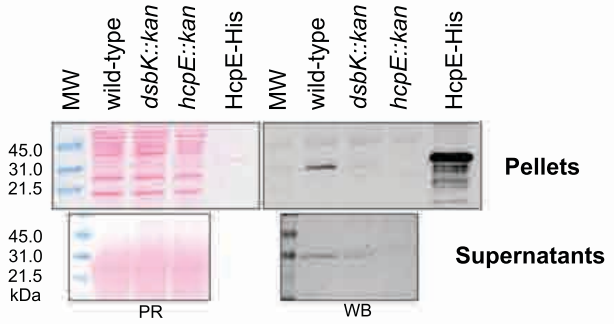

Lester et al Fig S3: Secretion of HcpE is also dependent on DsbK in strain SS1. SDS-PAGE analysis and anti-HcpE Western blotting of HcpE in total cells (top panels) or culture supernatants (bottom panels) of wild-type or *dsbK* or *hcpE* isogenic mutants shows decreased production and secretion of HcpE in the *dsbK* mutant. HcpE-His is purified recombinant protein that served as a positive control for Western blotting. PR: Ponceau red. WB: Anti-HcpE Western blot.

Lester et al Fig S4

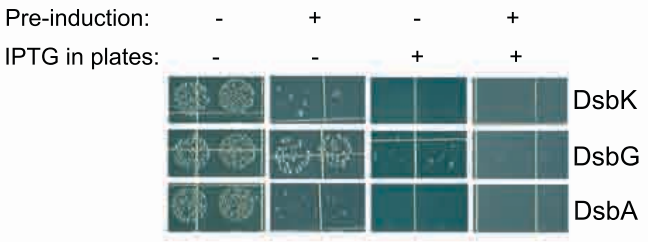

Figure S4: Effect of expresion of DsbK, DsbG and DsbA on bacterial growth in *E. coli*. *E. coli* BL21(DE3)pLys harbouring a pET vector for expression of either protein was pre-induced in broth for 3 h or not before being plated on LB agar containing IPTG or not. A 3h pre-induction was enough to highlight the toxicity of over-expression of DsbK and DsbA when plated on agar devoid of IPTG. Continuous over-expression on IPTG-containing agar was deleterious for all strains, notwithstanding pre-induction status.

Lester et al Fig S5

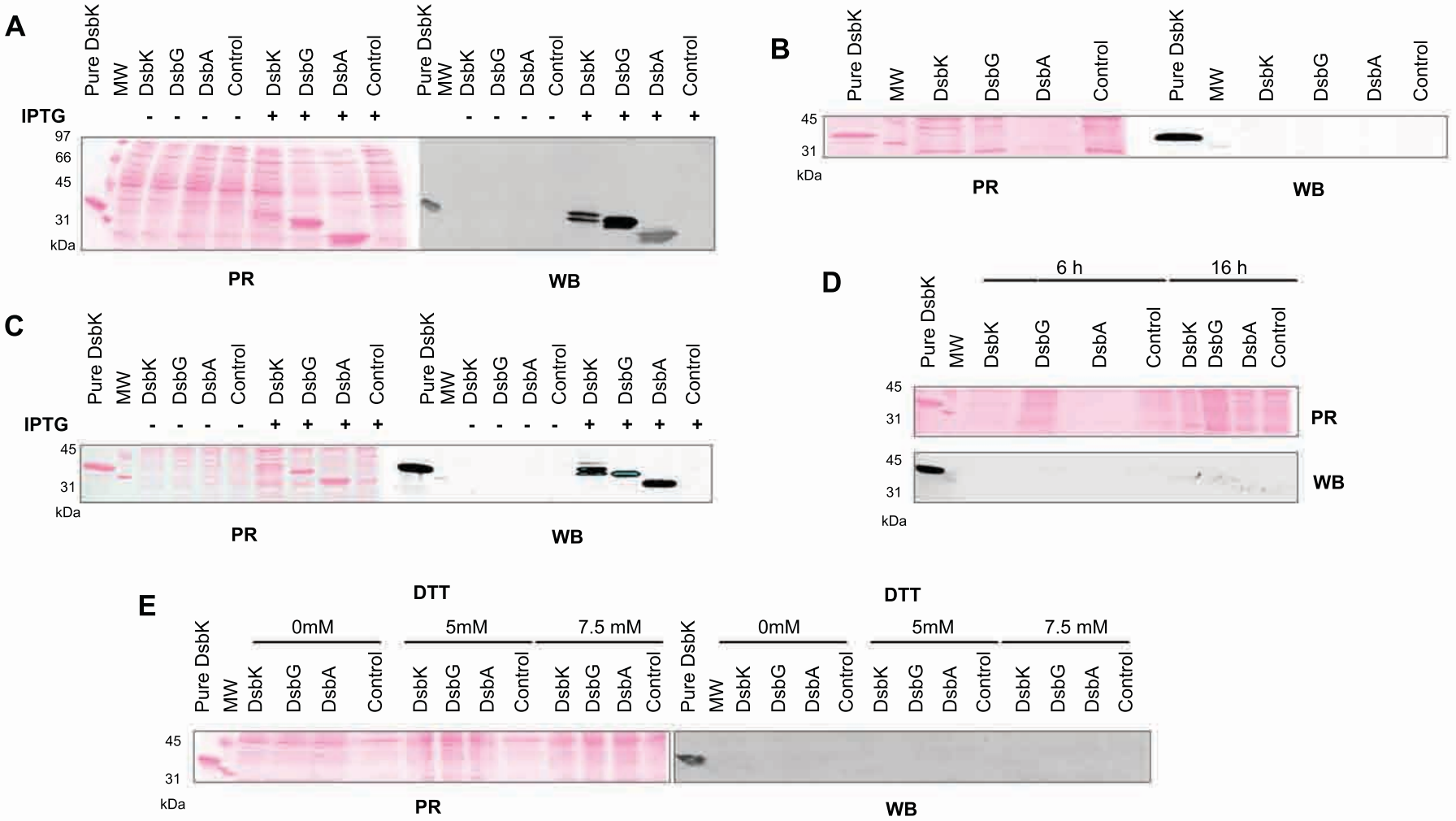

Figure S5: SDS-PAGE analysis of DsbK, DsbG and DsbA production in *E. coli* on plates or in broth after induction with IPTG and/or exposure to DTT. Detection was by Ponceau Red staining (PR) or anti-Histidine tag Western bloting (WB). The control protein was GMD, which is expressed at very low levels. Pure DsbK was used a positive control for Western blotting. **Panels A and C:** pre-induction for 3 h in broth prior to spot-plating (Panel A, cells used in Panel B) or prior to inoculation in broth (Panel C, cells used for Panels D and E). **Panel B:** analysis of cells scrapped off from plates after 16h. **Panels D and E:** analysis of cells recovered at 6 and 16 h after subculture in broth without (Panel D) or with DTT (Panel E).